Accepted Manuscript

P-T evolution of a spinel + quartz bearing khondalite from the Highland Complex, Sri Lanka: Implications for non-UHT metamorphism

P.L. Dharmapriya, S.P.K. Malaviarachchi, Andrea Galli, Ben-Xun Su, N.D. Subasinghe, C.B. Dissanayake, T.B. Nimalsiri, Bin Zhu

PII: S1367-9120(14)00208-9
DOI: http://dx.doi.org/10.1016/j.jseaes.2014.05.003
Reference: JAES 1946

To appear in: *Journal of Asian Earth Sciences*

Received Date: 10 February 2014
Revised Date: 30 April 2014
Accepted Date: 2 May 2014

Please cite this article as: Dharmapriya, P.L., Malaviarachchi, S.P.K., Galli, A., Su, B-X., Subasinghe, N.D., Dissanayake, C.B., Nimalsiri, T.B., Zhu, B., P-T evolution of a spinel + quartz bearing khondalite from the Highland Complex, Sri Lanka: Implications for non-UHT metamorphism, *Journal of Asian Earth Sciences* (2014), doi: http://dx.doi.org/10.1016/j.jseaes.2014.05.003

P-T evolution of a spinel + quartz bearing khondalite from the Highland Complex, Sri Lanka: Implications for non-UHT metamorphism

P. L. Dharmapriya[1, 2*], S. P. K. Malaviarachchi[2], Andrea Galli[3], Ben-Xun Su[4], N. D.Subasinghe[5], C. B. Dissanayake[5], T. B. Nimalsiri[1, 5], Bin Zhu [4, 6]

[1]Post Graduate Institute of Science, University of Peradeniya, 20400, Sri Lanka

[2]Department of Geology, Faculty of Science, University of Peradeniya, 20400, Sri Lanka

[3]Department of Earth Sciences, ETH Zurich, Sonnegstrasse 5, CH-8092 Zurich, Switzerland

[4]Institute of Geology and Geophysics, Chinese Academy of Sciences, 100029, Beijing, China

[5]Institute of Fundamental Studies, Hantana Road, Kandy, Sri Lanka

[6]University of Chinese Academy of Sciences, Beijing 100049, China

* Corresponding Author : P.L. Dharmapriya

E.mail address : dharmapriya1985@gmail.com

dharmapriyapdn@gmail.com

Postal Adders : Department of Geology, Faculty of Science, University of Peradeniya, 20400, Sri Lanka.

Mobile No : +94713317951

+94783451825

Abstract

Here, we report a natural field example for the coexistence of spinel+quartz within garnet-porphyroblasts as a non-UHT assemblage in a spinel- and cordierite-bearing garnet-sillimanite-biotite-graphite gneiss (khondalite) interbedded with orthopyroxene-garnet-biotite bearing intermediate granulites from the Highland Complex (HC) in Sri Lanka. The khondalite contains Zn-rich spinels mainly in four assemblage namely: (a) spinel co-existing with tiny quartz (ZnO = 12.67-12.85 wt%), (b) spinel surrounded by sillimanite moates and in intergrowth with skeletal sillimanites (ZnO = 9.03-9.17 wt%), (c) symplectitic spinels at the margin of sillimanite (ZnO = 4.09-4.28 wt%) and (d) spinelco-existing with ilmenite or as isolated grains (ZnO = 7.61-7.97 wt% and Cr_2O_3 = 5.99-6.27 wt%). Assemblage (a) and (b) occur within garnet while textures of (c) and (d) are present within cordierite moates after garnet in the matrix. Pseudosections calculated in the NCKFMASHTMnO system and conventional geothermobarometry suggest that the metamorphic peak conditions attained by the spinel+quartz bearing khondalites and associated intermediate granulites did not exceed T of 900 °C and P of 7.5-8.5 kbar. Post-peak evolution was characterized by a stage of nearly-isobaric cooling down to T of 770 °C and P of 7.5 kbar, followed by a late stage of isothermal decompression down to P < 6.5 kbar and T of 770 °C.

Thus, we propose that the incorporation of large amount of Zn into spinel from exotic, metasomatic fluids and possibly incorporation of Fe^{3+} into spinel under high oxidizing conditions may have shifted the stabilization of co-existing spinel+quartz to T < 900 °C. Hence, this study provides insights into the occurrence of spinel + quartz as a non- UHT assemblage suggesting that the coexistence of spinel + quartz should be treated with care and considered only as indicative, but not diagnostic of UHT metamorphism.

Key words: spinel+quartz assemblage, UHT metamorphism, Pseudosections, Highland Complex, Sri Lanka

1. Introduction

Aluminium and Magnesium rich granulites are essential to understand high-grade metamorphism, because they commonly preserve peak/near-peak mineral phases, including sapphirine, aluminous orthopyroxene, sillimanite, garnet, spinel or corundum, and display a range of post-peak reactions, which permit to unravel their P-T evolution (Droop and Bucher-Nurminen, 1984; Waters, 1986; Hensen, 1987; Droop, 1989; Su et al., 2012a). The mineral assemblage spinel + quartz has been documented from many well-known ultra-high-temperature (UHT) terrains across the globe and often used to infer extreme crustal UHT metamorphic conditions (e.g. Kawakami and Motoyoshi, 2004; Morimoto et al. 2004; Sajeev and Osanai, 2004b; Barbosa et al., 2006; Santosh et al., 2006; Tsunogae et al., 2008; Kawasaki et al., 2011; Zhang et al., 2012).

Despite the fact that spinel + quartz assemblage is reported from numerous UHT granulites, the influence of ZnO on the stability of spinel in the P-T space is still a matter of debate (Kelsey, 2008; Kawasaki et al., 2011). Many experimental studies have suggested that the stability of spinel + quartz assemblages may be shifted to lower temperatures and relatively higher pressures through the incorporation of Zn into spinel (e.g. Shultere and Bohlen, 1988; Nichols et al., 1992; Dasgupta et al., 1995; Das et al., 2001, 2003). Further, incorporation of minor elements such as Cr, Ti, Ni, V (Harley and Hensen, 1990; Waters, 1991; Nichols et al., 1992; Dasgupta et al., 1995; Harley 1998, 2008; Das et al. 2001; Kelsey 2008) or Fe^{3+} ions under oxidizing conditions (Hensen, 1986; Dasgupta et al., 1995) may strongly influence the stability field of spinel + quartz to lower temperatures.

This study was carried out in the Highland Complex (HC) Sri Lanka where evidences of UHT metamorphism have been reported only from few localities in the central HC and rarely in the southwestern part of the HC (Fig. 1) from the pelitic, mafic and quartzofeldspathic granulites (Osanai, 1989; Kriegsman and Schumacher, 1999;Osanai et al., 2000, 2003, 2006; Sajeev and Osanai, 2004a, 2004b; Sajeev et al., 2003, 2007, 2010).The reason for local occurrences of UHT granulites in the HC is still been a debate. In this paper, we report the P-T evolution of spinel- and cordierite-bearing garnet-sillimanite-biotite-graphite gneiss (khondalite) from the HC. Also we discuss the stability of field of direct co-existence of Zn-rich spinel with quartz within porphyroblastic garnets in the studied khondalite.

2. Geological setting

Based on Nd-model age determinations (Milisenda et al., 1988, 1994; Kröner et al. 1991), Proterozoic basement of Sri Lanka has been subdivided from the west to the east in four units (Kroner, 1991; Cooray, 1994, see Fig. 1): the Wanni Complex (WC), the Kadugannawa Complex (KC), the Highland Complex (HC) and the Vijayan Complex (VC).

The WC consists of amphibolite to granulite facies meta-sediments and meta-igneous rocks displaying Nd-model age of 1.1-1.8 Ma (Milisenda et al., 1988, 1994). The KC, often referred as "Arenas" (Vitanage, 1972; Almond, 1991), crops out in the northwestern part of the Kandy area and is composed of amphibolite to granulite facies basement rocks (Kröner et al., 1991; Cooray, 1994) with Nd-model ages ranging between 1.1 and 1.8 Ga (Milisenda et al., 1988, 1994). Some authors (e.g. Kehelpannala, 1997; Kroner et al., 2003) have suggested that the KC forms part of the WC based on geochronological, geochemical and structural evidences.

The basement of the centrally located HC yields Nd-model ages from 2.0 to 3.6 Ga (Milisenda et al. 1988, 1994). The HC is made of granulitic meta-quartzites, marbles, calcsilicates and metapelitic gneisses, intimately associated with charnockites (Cooray, 1962, 1984; Mathavan and Fernando, 2001). P-T conditions increase from 4.5-6 kbar and 600-700 ^{0}C in the southwestern part to 8-10 kbar and 800-900 ^{0}C towards the east (Faulhaber and

Raith, 1991; Schumacher and Faulhaber, 1994; Raase and Schenk, 1994; Mathavan et al. 1999; Kriegsman and Schumacher, 1999). Meta-sedimentary rocks such as marble and quartzite could be traced for more than 40 km in central and northeastern part of the HC, while thick bands of marble and quartzite in the southwestern parts of the HC are scarce (Mathavan et al. 1999). However, bands of wollastonite-scapolite, diopside- and scapolite-bearing granulites and cordierite-bearing gneisses occur in the SW part (Cooray, 1962, 1984; Hapuarachchi, 1968; Mathavan et al., 1999).

The VC yields Nd-ages of 1.1-1.8 Ga (Milisenda et al., 1988, 1994) and displays a suite of calc-alkaline orthogneisses, migmatites and minor meta-sedimentary enclaves such as meta-quartzite and calc-silicate rocks (Kehelpannala, 1997; Kröner et al., 2012) metamorphosed under upper amphibolite-facies.

During the last two and half decades, petrological, geochemical and geochronological studies on the HC have inferred, crustal UHT conditions of 925-1150 ^{0}C and 9-12.5 kbar (Osanai, 1989; Kriegsman and Schumacher, 1999; Osanai et al., 2000, 2003, 2006; Sajeev and Osanai, 2004a, 2004b; Sajeev et al., 2003, 2007, 2010) from very few localities. The age of the UHT event is still debated. From UHT granulites of the HC, Sajeev and Osanai (2003) have obtained the Sm-Nd isochron whole-rock age of 1478 ± 58 Ma, inferring that the UHT granulites could be relics of a pre-Pan African metamorphism. However, Sajeev et al. (2007) reported U-Pb zircon metamorphic age of ca. 580 Ma from relatively higher pressure UHT mafic granulites, which is in agreement with zircon and monazite ages of ca. 570 Ma determined from sapphirine granulites of the central HC (Sajeev et al., 2010), suggesting that the UHT granulites of the HC might have formed during assembly of the Gondwana super-continent.

3. Sample description and field relations

We collected spinel- and cordierite-bearing garnet-sillimanite-biotite-graphite gneisses (khondalite) and interbedded intermediate granulites exposed in an excavated embankment for construction close to the city of Horana. This area lies within the southwestern part of the HC and is mainly composed of cordierite-bearing metapelites, wollastonite-bearing calcsilicates, massive charnockites and charnockitic pegmatites (Cooray, 1965; Hapuarachchi, 1968). In our sampling area, quartzites, charnockites, khondalites, orthopyroxene-garnet-biotite gneisses, hornblende-biotite gneisses and pegmatites crop out intercalated with minor layers of marbles and calcsilicate gneisses (Fig. 2). The area displays a poly-phase ductile deformation history characterized by large scale folding and thrusting (Kehelpannala, 1997, 2003; Berger and Jayasinghe, 1976; Cooray, 1986; Sandifird et al., 1988; Voll and Kleinschrodt, 1991).The investigated khondalites are constituted of garnet, sillimanite, cordierite, plagioclase, alkali-feldspar, biotite and spinel with minor rutile, ilmenite and graphite. Zircon occurs as accessory mineral. Typically, garnet porphyroblasts are coarse-grained varying in size from 0.5 cm up to 8 cm (Fig. 3a and b) and are partly consumed by cordierite ± spinel moats (Fig. 3a). Rarely, coarse-grained calcite crystals are observed in plagioclase-rich domains. Khondalites display a strongly developed major foliation defined by compositional layering (Fig. 3c) and are interbedded and isoclinally folded together with dark colored layers of intermediate granulites (Fig. 3d). Intermediate granulite layers (30- 60 cm thick) are mainly composed of garnet, orthopyroxene, biotite, feldspars and quartz. Khondalite and intermediate granulites generally plunge gently with an attitude of N5^{0}E/25^{0}SE.

4. Petrography

4.1 Khondalite

The rock contains two petrographic domains: i) medium- to coarse-grained garnet-bearing (1-8cm in diameter) domain; ii) fine- to medium-grained garnet-bearing (0.25-1 cm) domain.

4.1.1 Textures of garnet porphyroblasts

Garnets in coarse to medium-grained garnet-bearing domain display numerous mono-phase and/or multi-phase inclusions of sillimanite, plagioclase, quartz, alkali-feldspar and less abundantly cordierite, spinel, ilmenite, rutile, biotite, zircon, monazite and tourmaline. Spinel inclusions occur two types: i) spinel directly coexisting with tiny quartz in mantle area of garnet, commonly surrounded by coarse-grained alkali-feldspar and associated with light brownish biotite flakes (Fig. 4a, b and c), and ii) spinel surrounded by sillimanite moats (Fig. 4d, e) or in intergrown with skeletal sillimanite ± alkali-feldspar (Fig. 4f) in the mantle area of garnet. The sillimanite grains present from the core to the rim area of garnet are considered as prograde and sillimanite moats and skeletal sillimanite found around spinel from the mantle to rim of garnet are probably formed during retrogression (Fig. 4d-g). Tiny tourmaline inclusions areobserved at the mantle area of spinel- and quartz-bearing garnet-porphyroblasts (Fig. 4h).

Isolated anhedral plagioclase, alkali-feldspar and biotite inclusions occur widespread from the mantle to the rim of garnet. Quartz inclusions are less abundant especially in spinel-bearing garnets. Occasionally, tiny quartz inclusions (<0.1mm) can be recognized close to where sillimanite-spinel aggregates occur (Fig.4g). In spinel-free garnets, quartz inclusions occur up to 1 cm in size. Cordierite inclusions are commonly observed along fractures from rim to lower mantle area of coarse garnet (Fig. 4i).

Garnet in fine- to medium-grained garnet bearing domain contains quartz, plagioclase, biotite and sillimanite as major inclusion phases. Rutile and ilmenite occur as minor inclusions, while zircon and apatite occur as accessory inclusion phases (Fig. 4j).

4.1.2 Textures of Matrix minerals

Most of the garnets in medium- to coarse-grained garnet-bearing domain are rimmed by cordierite ± spinel, sillimanite and quartz (Fig. 4k-o). Stretched quartz (up to 5cm in length), prismatic sillimanite (0.5-1.5cm), subhedral and anhedral two feldspars, acicular biotite, anhedral porphyroblastic cordierite (0.5-1.5cm), coronitic cordierite after garnet and minor graphite flakes form the main mineral assemblage in the matrix. The preferred orientation of quartz, prismatic sillimanite, biotite and graphite flakes define the main rock lineation on major foliation (Fig. 4p). Spinel inclusions found in cordierite occur in two textural types: i) spinel embedded as isolated grains or together with ilmenite, adjacent to sillimanite and quartz (Fig. 4l and m); ii) symplectitic spinel at the margin of sillimanite (Fig. 4n and o).

In fine- to medium-grained garnet-bearaing domains, the matrix is composed of prismatic sillimanite, two feldspars, stretched quartz, anhedral cordierite and acicular biotite, with minor amount of graphite (Fig. 4q). Garnets of this domain do not show any breakdown reactions.

4.2 Intermediate granulites

The dark colored intermediate granulites contain anhedral orthopyroxene (0.25-1 cm in size), plagioclase and alkali-feldspar (0.25 to 1.5 cm in size), medium- to fine-grained quartz and acicular biotite as major constituents, anhedral garnet (0.25 to 3 cm in size) and ilmenite as minor minerals, and rutile, apatite and zircon as accessory (Fig. 4r - t). Biotite in this rock are found as two modes: (a) acicular coarse to medium biotite flakes which always show prefer orientation have sharp grain margins (Fig. 4r and s). Occasionally, this biotite which can be observed as inclusions and/or partial inclusion phase with in garnet and orthopyroxenes can be considered as a peak metamorphic mineral. (b) Medium to fine anderdal biotite which are mostly associated at the margins of orthopyroxene and garnets and always shows random orientation (Fig. 4r – t). These biotites do not have sharp grain margins and could be a retrograde product due to hydration of orthopyroxene and garnet.

Other than the biotite, garnet contains quartz and plagioclase as major inclusion phases while alkali-feldspar, rutile and ilmenite as minor phases. Tiny quartz and plagioclase inclusions can be observed in orthopyroxenes with biotite (Fig. 4s).

5. Whole rock and mineral chemistry

5.1 Whole rock chemistry

Major and trace element compositions of the khondalite and intermediate granulites are taken from XRF analysis, performed using a Panalytical Axios wave-length dispersive XRF spectrometer (WDXRF, 2.4 kV) at the ETH Zurich, Switzerland. The obtained major and trace element data are presented in Table. 1.

Both khondalite and intermediate granulites show high Si (up to 57.2 wt % and 56.8 wt %, respectively). Khondalite is Al-richer than interbedded intermediate granulite (20.2 wt % vs. 14.8 wt %). X_{Mg} of the two types of granulite are 0.27 and 0.41, respectively. Both khondalite and intermediate granulites display high Rb, Ba, Zr, Zn, Cr and V contents (Table.1).

5.2 Mineral chemistry

Chemical analyses of the khondalite were carried out using JEOL JXA8100 electron probe microanalyzer (EPMA) at Institute of Geology and Geophysics, Chinese Academy of Sciences, at Beijing, China. All analyses were operated at an accelerating voltage of 15 kV and 10 nA beam current, 3 μm beam spot and 10-30 s counting time on peak. Natural (jadeite

[$NaAlSiO_6$] for Na, Al and Si, rhodonite [$MnSiO_3$] for Mn, sanidine [$KAlSi_3O_8$] for K, garnet [$Fe_3Al_2Si_3O_{12}$] for Fe, Cr-diopside [$(Mg, Cr)CaSi_2O_6$] for Ca, olivine [$(Mg, Fe)_2SiO_4$] for Mg) and synthetic (rutile for Ti, 99.7% Cr_2O_3 for Cr, Ni_2Si for Ni) minerals were used for standard calibration (Su et al. 2012b), and a program based on the ZAF procedure was used for matrix corrections. The precisions of all analyzed elements are better than 98.5%.

5.2.1 Spinel

Spinels included in garnet-porphyroblasts display relatively high X_{Mg} values of 0.41-0.43 (Table 2). They are also rich in ZnO (12.67-12.85 wt%) and poor in Cr_2O_3 (0.77-0.80 wt%). Spinels mantled by sillimanite within garnet have an X_{Mg} of 0.38-0.39, ZnO and Cr_2O_3 contents of 9.03-9.17 wt% and 0.20-0.29 wt%, respectively. Isolated spinels associated with cordierite show relatively low X_{Mg} values of 0.27-0.29, ZnO contents of 7.61-7.97 wt% and relatively high Cr_2O_3 of 5.99-6.27 wt%. Symplectitic spinels at the margin of sillimanite have X_{Mg} of 0.31-0.32, relatively low ZnO contents (4.09-4.28 wt%) and Cr_2O_3 contents of 0.71-1.61 wt%.

5.2.2 Garnet

Garnet shows almandine-pyrope solid solution (X_{Alm}:58.7-60.0 and X_{Prp}: 32.8-36.0), with little amounts of grossular (X_{Grs}<0.015) and spessartine (X_{Sps}<0.025) components (Table 3). The porphyroblasts are slightly zoned, showing increasing X_{Mg} and X_{Ca} while decreasing X_{Fe} and X_{Mn} from the core towards the rim (Fig. 5).

5.2.3 Cordierite

Cordierites in moats surrounding garnet and inclusions in garnet have relatively high X_{Mg} of 0.77 and display low Na_2O contents <0·02 wt%. Total oxides of cordierite yield about 98 wt%, indicating minor channel-filling volatiles such as CO_2 and/or H_2O (Table 3).

5.2.4 Biotite

Biotite composition varies with textural settings (Table 3). Biotite in contact with composite spinel + quartz inclusions within garnet displays an X_{Mg} of 0.79-0.80 and a TiO_2 content of 2.94-3.02 wt%. Isolated biotite inclusions in garnet have slightly lower X_{Mg} value of 0.74 and high TiO_2 content of 5.92 wt%, while biotite in contact with garnet and cordierite moats show X_{Mg} of 0.66 and TiO_2 contents of 3.14-3.53 wt%.

5.2.5 Feldspars

Matrix plagioclase is Ca-poor, having a X_{An} of 0.29. Both matrix alkali-feldspar and alkali-feldspar inclusions surrounded by spinel + quartz assemblage and sillimanite in garnet-porphyroblasts have composition of X_{Or} of 0.89and 0.86, respectively (Table 3).

5.2.6 Ilmenite

MnO content of ilmenite is relatively high (0.25-0.31 wt%, Table 3), while X_{Mg} up to 0.048. The calculated Fe^{3+} component from ilmenite grains within cordierite moats around garnet is 0.039. Ilmenite inclusions within mantle area of garnet display higher Fe^{3+} content of 0.062, indicating high oxidising conditions during garnet growth.

6. Textural evolution

6.1 Khondalite

Mineral assemblage(s) preserved as inclusions in large porphyroblasts, commonly garnet, may preserve at least part of the prograde evolution of a rock. In the studied khondalite, spinel + quartz inclusions within garnet completely surrounded by alkali-feldspar (Fig. 4a and b), together with Ti-rich biotite and rare sillimanite inclusions within alkali-feldspar grains located next to spinel may suggest the occurrence of the prograde reaction:

$$Bt + Sil = Spl + Qtz + Kfs + Melt \quad (1)$$

Above minerals together with rutile inclusions in garnet may indicate that the peak mineral assemblage of the studied samples consist of spinel-quartz-sillimanite-plagioclase-alkali-feldspar-biotite-garnet as major phases and rutile as a minor phase.

Spinel rimmed by skeletal sillimanite grains within mantle areas of garnet-porphyroblasts indicates the breakdown of spinel + quartz peak assemblage during cooling via the reaction:

$$Spl + Qtz = Grt + Sil \quad (2)$$

In the studied sample, the lack of quartz associated with this particular texture could suggest that quartz has been completely consumed during the reaction, as also reported by Kawakami and Motoyoshi (2004) from garnet-sillimanite leucogneisses of the Lutzow-Holm Complex in East Antarctica.

Formation of cordierite ± spinel moats surrounding garnet-porphyroblasts in the presence of sillimanite ± quartz and ilmenite probably result from the following pressure-sensitive reactions:

$$Grt + Sill + Qtz = Cord \pm Spl \quad (3)$$

Grt + Sill = Cord + Spl   (4)

These reactions may have taken place during near isothermal decompression.

6.2 Intermediate granulites

The peak assemblage orthopyroxene-garnet-biotite-quartz-plagioclase-alkali-feldspar observed in the intermediate granulites probably formed through a series of fluid-absent prograde biotite melting reactions such as

Qtz + Bt = Opx + Kfs + Melt (5)

Qtz + Bt = Grt + Kfs + Melt   (6)

Qtz + Bt = Grt + Opx + Kfs + Melt   (7)

Qtz + Pl + Bt = Grt + Opx + Kfs + Melt   (8)

which partly consumed quartz and biotite from the rock matrix and produced orthopyroxene, garnet and alkali-feldspar as peritectic melting phases. Reactions (5) to (8) may explain the occurrence of tiny quartz, plagioclase and biotite inclusions commonly observed in orthopyroxene and garnet (Fig. 4s and t). The preservation of biotite and quartz in the matrix suggests that temperatures during melting were not sufficiently high to completely consume the reactants of reactions (5) to (8). As experimentally shown by Vielzeuf and Montel (1994), biotite-quartz-orthopyroxene-garnet-melt coexist over a 50-100 °C wide multivariant field, in which by increasing T the proportion of biotite-quartz decrease and those of orthopyroxene-garnet increase, respectively, before the melting reactions go to completion.

7. P-T estimates

In order to estimate peak metamorphic conditions of the studied khondalite, we applied two complementary approaches: pseudosections and conventional geothermobarometry. The pseudosection approach is independent from mineral compositions that may have been modified during cooling. Nevertheless, the lack of thermodynamic data to include Zn in the modeling and hence to quantify its role on the stability of spinel, which is the crucial phase of the investigated khondalite, may represent a major drawback. However, using experimentally calibrated geothermobarometers complementarily, such as the Ti-in-Garnet geothermometer (e.g. Kawasaki and Motoyoshi, 2007), the Ti-in-Biotite thermometer (Henry et al., 2005) and the GASP geobarometer (e.g. Koziol and Newton, 1988) may fill the void, due to the fact that these calibrations are non spinel-related and only slightly dependent on Fe-Mg exchange. Therefore, they should not be strongly influenced by compositional modifications due to reverse diffusion, as commonly observed in high-grade rocks after peak metamorphism.

We constructed pseudosections for both the khondalite and interbedded intermediate granulites in the chemical system of NCKFMASHTMnO, the most reliable system approximating the real composition of natural rocks that we can actually model, using the software Perplex_X_07 (Connolly, 2005), the 2004 update of the Holland and Powell (1998) internally-consistent thermodynamic database and mineral solution models as listed in the caption to the Fig. 6. The modeled bulk rock compositions are taken from XRF analysis. We neglected P_2O_5 from the calculations, and therefore the CaO content equivalent to apatite was extracted from the measured bulk composition. H_2O content corresponds to the loss on ignition (LOI). In order to investigate the oxidation state of the samples and have an estimate of their Fe_2O_3 content we calculated *T*-*X*(Fe_2O_3) pseudosections at pressure of 8.0 kbar (Fig. 6a and c).

In the T-X(Fe_2O_3) section calculated for the khondalite (Fig. 6a), spinel + quartz coexist with sillimanite at *X*(Fe_2O_3) between 0.07 and 0.42, and temperatures ranging between 1000 °C and 1060 °C. At higher T, sillimanite is predicted to disappear, while at lower T spinel would not be stable, for *X*(Fe_2O_3) < 0.16, or be replaced by magnetite. Since in the studied sample magnetite is absent, we suggest that the *X*(Fe_2O_3) value which indicate the oxidation state of the rock has to be located between 0.07 and 0.16.

The P-T pseudosection of Fig. 6b, calculated at *X*(Fe_2O_3) = 0.10, represents the stability of coexisting minerals for the composition of the studied khondalite in the *P*-*T* space. Spinel and quartz coexist at temperatures > 925 °C and pressures comprised between 5 and 8 kbar (see bold field in Fig. 6b), while their occurrence together with sillimanite is restricted to temperatures of 965-1065 °C and pressures of 7-8 kbar. At higher T and lower P, sillimanite would disappear and cordierite and orthopyroxene would be stable; at higher P, spinel would disappear. Nevertheless, the modeling failed to reproduce the observed peak mineral assemblage because Spl + Qtz (+ Grt, Sil, Pl, Kfs) are never predicted to coexist with biotite, whose stability is limited at T < 890 °C (see dashed line in Fig. 6b). At higher T, biotite would be completely consumed through biotite melting reactions.

In many granulite terrains, layers of intermediate granulites composed of opx-garnet-biotite gneisses interbedded within metapelites are common and are generally interpreted as metagreywackes (e.g. Asiedu et al., 2004; Saxena and Pandit, 2012). Since, major element compositions similar to those of the investigated intermediate granulites (Table. 1) have been reported from matagreywake of the Birim diamondiferous field, southern Ghana (Asiedu et al., 2004) and from the Hindoli Group metasediments, SE Aravalli Craton, NW India (Saxena and Pandit, 2012), while Asiedu et al. (2004) have described similar trace element compositions from metagreywakes of Birim diamondiferous field, southern Ghana. This suggests that khondalite and intermediate granulites form a meta-sedimentary suite metamorphosed to granulite-facies conditions. Therefore, modeling of the intermediate granulites interbedded with khondalites may avoid the discrepancy of Zn in the modelling, because spinel is not part of the stable assemblage and thus the *P-T* estimate is not spinel (+ quartz) dependant. The *T*-*X*(Fe_2O_3) section calculated at P = 8 kbar and *X*(Fe_2O_3) ranging between 0 and 0.2 (Fig. 6c) displays the effect of minor amount of ferric iron on the phase relations. The peak assemblage Opx-Bt-melt-Pl-Kfs-Grt-Qtz-Ilm is stable for *X*(Fe_2O_3) < 0.08 at T around 900 °C. The occurrence of Cpx at higher X(Fe_2O_3) delimitates the maximum bulk ferric iron content, while the appearance of clinopyroxene at T < 885 °C and the disappearance of biotite at T > 910 °C bound the temperatures.

In the *P-T* pseudosection of Fig. 6d calculated at *X*(Fe_2O_3) = 0.01, the disappearance of biotite and the appearance of alkali-feldspar confines the peak temperature at around 900 °C. The peak pressure is delimited at about 7-8 kbar by the appearance of Cpx at higher P. This estimate matches well the results of melting experiments on metagreywackes (e.g. Vielzeuf and Holloway, 1988; Vielzeuf and Montel, 1994; Clemens et al. 1997), which shows that at around 8 kbar biotite-orthopyroxene-garnet-quartz-plagioclase-alkali-feldspar coexist between 860 °C and 930 °C (Vielzeuf and Montel, 1994).

Estimated peak conditions from *P-T* pseudosections are compared with conventional geothermobarometric calculations. Mineral compositions in Table1, 2 and 3 are used in the calculations and a summary of the results are given in Tables 4. The Ti-in-Garnet geothermometer of Kawasaky and Motoyoshi (2007) using garnet core-composition yielded temperature of 860 °C. The Ti-in-Biotite thermometer of Henry et al. (2005) yield slightly lower temperature of 828 °C, assuming no ferric iron in the biotite structure. However, the estimated temperatures would increase up to 834 °C and 841 °C considering the incorporation of 10% and 20% ferric iron into biotite, respectively. The Koziol and Newton (1988) calibration of the GASP geobarometer yields pressures of 7.3, 7.7, 8.0, 8.3 and 8.6 kbar at nominal temperatures of 800, 825, 850, 875 and 900 °C, respectively.

Decreased cation diffusion rates at lower temperatures may lead to the development of micro-scale volumes of equilibration in rocks. Hence, the use of pseudosections in the investigation of post-peak evolution may be misleading due to the difficulty of estimating the effective bulk composition related with a specific reaction (e.g. Galli et al., 2010). Alternatively, we reconstructed the post-peak evolution of the sample by calculating the P-T conditions of relevant reactions observed in thin section (Tables 2 and 3).

The reaction (2) observed in the mantle area of garnet-porphyroblasts from the khondalite (Fig. 4d-g), (experimentally investigated by Nichols et al. (1992) in the system FMASZn), yields post-peak temperatures of 810 and 830 °C for pressures of 7.7 and 8.2 kbar, respectively, suggesting that a period of isobaric cooling occurred after metamorphic peak (Fig. 7).

Intersection of the reaction 3 (experimentally calibrated by Wells and Richardson, 1980 and Holdaway and Lee, 1977) with the Garnet-Cordierite thermometer of Bhattacharya et al. (1988) occurs at temperatures of about 765-770 °C and pressures of 6.5-7.0 kbar, in good agreement with the Spinel-Cordierite thermometer of Das et al. (2003), calculated for spinel-cordierite moats around garnet yielding T of about 770 °C (Fig. 7). Similar temperatures of 770-780 °C are estimated using the Ti-in-Biotite thermometer of Henry et al. (2005) for late biotite crystallized at the margin of garnet-porphyroblasts. The P-sensitive reaction (3) suggests that after isobaric cooling the khondalite may have experienced a late stage of nearly isothermal decompression (Fig. 7). A decrease in pressure is also demonstrated by the occurrence of ilmenite as oxide phase commonly associated with late cordierite ± spinel-bearing moats and coronas. Further this could be explained by the decreasing almandine and spessartite components and increasing pyrope and grossular components from core to rim observed in zoned garnet-porphyroblast (Fig. 5).

8. Discussion

Spinel and quartz may mislead many to interpret non-UHT textures as UHT features. For example, textures such as spinel-quartz inclusions in garnet porphyroblasts where the quartz is a late crystallization product formed from either melt rather than part of an equilibrated assemblage, or post-peak decompositions of magnetite-ulvospinel solid solution (Harley, 2008). Therefore, care must be taken in the interpretation of *P-T* evolution of Zn-rich spinel in equilibrium with quartz.

8.1 Formation of Zn-rich spinels and variation of oxygen fugacity (f_{O2}) during the evolution of khondalite

The formation of Zn-rich spinel in pelitic rocks is commonly explained by: i) breakdown of Zn-rich silicates such as staurolite (e.g. Stoddard 1979; Gallien et al., 2010) and biotite (e.g Shabeer et al., 2002; Morimoto et al. 2004; Santosh et al., 2006) or ii) metasomatic fluids carrying excess ZnO (and MgO) into the rock (e.g. Ogo et al., 1992). In the first case, during prograde metamorphism staurolite dehydrates and Zn can incorporate into minerals containing Fe^{2+} in the tetrahedral coordination such as spinel (e.g. Loomis 1972; Stoddard 1976). Ogo et al. (1992) and Hiroi et al. (1994) reported Zn-rich hercynite (ZnO up to 10.79 wt%) together with Zn-rich staurolite (ZnO up to 2.25 wt%) in kyanite-staurolite-garnet-bearing khondalites from the southwestern part of the HC. Zn-rich staurolite (ZnO up to 2.14 wt%) from the HC have been also described by Rasse and Schenk (1994). Nevertheless, the khondalites investigated in this study are lack of staurolite. Thus, formation of Zn-rich spinel via staurolite breakdown seems to be unlikely. Consumption of Zn- and Cr-rich biotite during prograde metamorphism may lead to formation of Zn-rich spinel, as inferred by Morimoto et al. (2004) from UHT khondalite in southern India. However, in the present study the ZnO and Cr_2O_3 contents of biotite associated with sipinel + quartz assemblage range between 0.07-0.12 wt% and 0.31-0.40 wt%, respectively. Therefore, destabilization of biotites can only contribute in minor amount to increase the Zn content in spinel of the studied khondalites.

Alternatively, formation of Zn-rich spinel could be explained by infiltration of chemically active fluids under high f_{O2}. Presence of ilmenite with relatively high Fe^{3+} content close to spinel grains coexisting with quartz and ilmenite inclusions within alkali-feldspar which encloses spinel + quartz assemblage (Fig. 4b) suggests high oxidizing condition may have prevailed during formation of spinel + quartz. Distribution of ilmenite grains at garnet margin (Fig. 4n), within cordierite (Fig. 4k to n) and close to retrograde spinels (Fig. 4i and m) may indicate that high oxidizing conditions existed even during the post-peak isothermal decompression. Rare tourmaline inclusions within garnet porphyroblasts associated with spinel + quartz could also suggest that metasomatic fluids may have entered into the system during the rock's evolution. Such chemically active fluids may have added ZnO, BO_3 and Cr_2O_3 from exotic sources forming tourmaline and/or Zn- and Cr-rich spinel (e.g. Ogo et al.,1992). Addition of exotic Zn and Cr is also inferred by the Zn- and Cr-rich compositions of post-peak spinels which may have formed via reactions (3) and (4). Moreover, the reactants, garnet, sillimanite and quartz, as well as the surrounding plagioclase, alkali-feldspar and ilmenite, show lower ZnO and Cr_2O_3 contents than the produced spinel. Hence, it is suggested that Zn- and Cr-rich spinel are formed by addition of metasomatic fluids into the khondalite of the HC.

Figure 8 compares the Zn content (p.f.u) vs. X_{Mg} of spinel associated with quartz in the present study and other high-grade terrains worldwide. It clearly demonstrates that the stability of Zn-rich spinel + quartz is not univocally correlated in the P-T space with the Zn content of spinel since Zn-rich spinel co-existing with quartz has been reported from a wide spectrum of P-T conditions, ranging between 6-12 kbar and 830-1000 ^{0}C, respectively.

In the investigated sample, the stabilization of coexisting spinel + quartz at < 900 °C seems to result from the combined incorporation of considerable amount of Zn (up to 12.85 wt% of ZnO) and Fe^{3+} into spinel under relatively high oxidizing conditions during peak metamorphism. In fact, the calculated T-$X(Fe_2O_3)$ section (Fig. 6a) predicts that the observed mineral assemblage requires $X(Fe_2O_3)$ of 0.07-016 to be stable.

8.2 P-T evolution of the HC khondalite

In Fig. 7 we present a possible *P-T* path for the investigated HC khondalite and interbedded intermediate granulite. Both pseudosection and conventional geothermobarometric calculations suggest that peak metamorphic condition occurred at temperatures of 870-900 ^{0}C and pressures of 7.5-8.5 kbar. Textural observations coupled with geothermobarometric estimates indicate that after the metamorphic peak the HC khondalite has been subjected to a phase of isobaric cooling (as inferred from reaction 2) followed by a phase of nearly isothermal decompression (shown by reactions 3 and 4).

Thus, this study presents clear evidence showing that spinel + quartz assemblage bearing khondalite of the south western HC, Sri Lanka, has not reached UHT conditions during its metamorphic evolution. Generally proposed P-T conditions for the southwestern part of the HC are 600-750 ^{0}C and 4.5-6 kbar (e.g. Mathavan et al., 1999), which is approx. 2-3 kbar and 200-250 °C less than the conditions suggested by this study. Raase and Schenk, (1994) have proposed that the both southeastern and southwestern parts of the HC together comprise ~15 km thick slice of the deep crust from about 30-35 km depth in the southeast to 15- 20 km depth in the west suggesting that the lower crustal cross-section exposed in the HC was already tilted during cooling.

However, the occurrence of rare kyanite inclusions in garnet in pelitic granulites (Hiroi et al., 1987, 1994; Ogo et al., 1992), osumilite and spinel + quartz-bearing UHT pelitic granulites (Sajeev and Osanai 2004b) and spinel + quartz assemblage in non UHT pelitic granulites presented in this study, arise the necessity to reinvestigate the regional geology of the southwestern HC.

In comparison, the southern Indian granulite terrain which is the nearest granulite terrain to the HC, metamorphosed simultaneous with the HC during the final phase of the assembly of Gondwana (Braun et al., 1998; Santosh et al., 2003, Collins et al., 2007) also contains spinel+quartz assemblage in khondalite (Morimoto et al., 2004) and garnet–orthopyroxene–cordierite granulites (Shimizu et al., 2009). However, those rocks have been interpreted to be metamorphosed under UHT conditions.

9. Conclusions

Petographical and two complementary geothermobarometric approaches (pseudosections and conventional geothermobarometry) reveal that peak metamorphic mineral assemblage of the studied khondalite from the southwestern HC, Sri Lanka, comprised of Zn-rich-spinel + quartz assemblage. The rock has records of maximum *P-T* conditions of 7.5-8.5 kbar and 870-900 ^{0}C, respectively, thus has not reached UHT metamorphic conditions. Coexistence of spinel + quartz at T < 900°C is imputed to the incorporation of high amount of Zn (up to 12.85 wt%) and Fe^{3+} contents under high oxidizing conditions. High Zn content of spinel along with enrichment of Cr in some retrograde spinel together with Zn and Cr poor nature of reactants (garnet, sillimanite and quartz) and matrix minerals (plagioclase, alkali-feldspar and ilmenite) provide clues to involvement of Zn and Cr rich metasomatic fluids.

Therefore, the current study provides a natural field example showing the occurrence of spinel + quartz assemblage as a non- UHT assemblage suggesting that the coexistence of spinel + quartz assemblage should be treated with care and considered only as indicative, but not diagnostic of UHT metamorphism. Further, the examined khondalite also highlights the limitations of pseudosections in the modeling of Zn-rich spinel bearing rocks. Hence, the best approach to deal this drawback is probably to calculate pseudosections of samples which share the same metamorphic history but of different bulk compositions (e.g. khondalite vs. intermediate granulites) and compare the results with those from non spinel-related conventional geothermobarometers.

Acknowledgements

We are grateful to the National Research Council (NRC) of Sri Lanka (Grant No.NRC-11-180) and the National Natural Science Foundation of China (Grant No. 41173011) for funding this project. Our thanks are due to L.R.K. Perera of the Department of Geology, University of Peradeniya and to J. Connolly from the ETH Zurich for constructive comments during the study. We thank S. Opatha and Thilini Harischandra at the Institute of Fundamental Studies (IFS) for technical advice and support in preparing petrographic thin sections, respectively. We also appreciate Qian Mao and Yuguang Ma at Institute of Geology and Geophysics, Chinese Academy of Sciences for EPMA analysis.

References

Almond, D. C., 1991.Arena Gneiss and Kandy Gneiss-a proposed subdivision of the Highland Series around Kandy, and its significance. Journal of Geological Society of Sri Lanka, **3**, 41-50.

Andersen, D. J., Lindsley, D. H. & Davidson, P.M., 1993. QUILF: a PASCAL program to assess equilibria among Fe–Mg–Mn–Ti oxides, pyroxenes, olivine, and quartz.Computers and Geosciences, **19**, 1333-1350.

Asiedu, D. K., Dampare, S. B., Asamoah Sakyi, P., Banoeng-Yakubo, B osae, S., Nyarko, B. J. B. & Manu, J., 2004. Geochemistry of Paleoproterozoic metasedimentary rocks from the Birim diamondiferous field, southern Ghana: Implications for provenance and crustal evolution at the Archean-Proterozoic boundary. Geochemical Journal, **38**, 215 – 228.

Barbosa, J., Nicollet, C., Leite, C., Kienast, J. R., Fuck. & R. A., Macedo, E.P., 2006. Hercynite–quartz-bearing granulites from Brejões Dome area, Jequié Block, Bahia, Brazil: influence of charnockite intrusion on granulite facies metamorphism. Lithos, **92,** 537-556.

Berger, A. R. & Jayasinghe, N. R., 1976.Precambrian structure and chronology in the Highland Series of Sri Lanka. Precambrian Research, **3**, 559-576.

Bertrand, P., Ellis, D. J.& Green, D.H., 1991. The stabitlity of sapphirine-quartz and hypersthenes-sillimanite-quartz assemblage: an experimental investigation in the system

FeO-MgO-Al_2O_3-SiO_2 under H_2O and CO_2 conditions. Contributions to Mineralogy and Petrology, **108**,338-344.

Bhattacharya, A., Mazumdar, A. C. & Sen, S. K., 1988. Fe-Mg mixing in cordierite: Constraints from natural data and implications for cordierite-garnetgeothermometry in granulites. American Minerelogists, **73**, 338-344.

Bohlene, S. R., Dollase, W. A. & Wall. V.J., 1986. Calibration and applications of spinel equilibria in lhesystemFeO-Al_2O_3,-SiO^2. Journal of Petrology, **27**, 1143-1156.

Braun, I., Montel, J.M. & Nicollet, C., 1998. Electron microprobe dating monazites from high-grade gneisses and pegmatites of the Kerala Khondalite Belt, southern India. Chemical Geology **146**, 65–85.

Connolly, J. A. D., 2005. Computation of phase equilibria by linear programming: a tool for geodynamic modelling and its application to subduction zone decarbonation. Earth and Planetary Sciences Letters, **236**, 524-541.

Collins, A.S., Santosh, M., Braun, I. & Clark, C., 2007. Age and sedimentary provenance of the Southern Granulites, South India: U–Th–Pb SHRIMP secondary ion mass spectrometry. Precambrian Research **155**, 125–138

Clemens, J. D., Droop, G. T. R & Stevens, G., 1997. High-grade metamorphism, dehydration and crustal melting: a reinvestigation based on new experiments in the silica-saturated portion of the system $KAlO_2$-SiO_2-H_2O-CO_2 at P• 1.5GPa. Contributions to Mineralogy and Petrology, **129**, 308-325.

Cooray, P. G., 1962. Charnockites and their associated gneisses in the Precambrian of Ceylon.Journal of Geology Society, London,**118**, 239- 273.

Cooray, P. G., 1965. The Geology of the Country around Alutgama.Ceylon Geology. Survey Department, Museum., 3, 111.

Cooray, P. G., 1984. An introduction to the geology of Sri Lanka. National Museum Sri Lanka, 340.

Cooray, P. G., 1986. A note on recumbent folding in the central Highlands of Sri Lanka. Geolical Society of Sri Lanka, L.J.D. Fernando Felicitation Volume, 101 - 107.

Cooray, P. G., 1994. The Precambrian of Sri Lanka: a historic review. PrecambrianResearch, **66**, 3-18.

Das, K., Dasgupta, S., & Miura, H., 2001. Stability of osumilite coexisting with spinel solid solution in metapelitic granulites at high oxygen fugacity. American Mineralogist, **86**, 1423-1434.

Das, K., Dasgupta. S. & Miura, H., 2003. An experimentally constrained petrogenetic grid in the silica-saturated portion of the system KFMASH at high temperatures and pressures. Journal of Petrology, **44**, 1055-1075.

Dasgupta, S., Sengupta, P., Ehl, J., Raith, M. & Bardhan, S., 1995. Reaction textures in a suite of spinel granulites from the Eastern Ghats Belt, India: evidence for polymetamorphism, a partial petrogenetic grid in the system KFMASH and the roles of ZnO and Fe_2O_3. Journal of Petrology, **36**, 345-461.

Diener J. F. A., Powell, R., White, R. W. & Holland, T. J. B., 2007.A new thermodynamic model for clino- and orthoamphiboles in the system Na_2O-CaO-FeO-MgO-Al_2O_3-SiO_2-H_2O-O.Journal of Metamorphic Geology, **25**, 631-56.

Droop, G. T. R. & Bucher-Nurminen, K., 1984. Reaction textures and metamorphic evolution of sapphirine-bearing granulites from the Gruf Complex, Italian Central Alps. Journal of Petrology, **25**, 766-803.

Droop, G. T. R., 1989. Reaction history of garnet–sapphirine granulites and conditions of Archaean high-pressure granulite facies metamorphism in the Central Limpopo Mobile Belt, Zimbabwe. Journal of Metamorphic Geology, **7**, 383-403.

Faulhaber, S. & Raith, M., 1991. Geothermometry and geobarometry of high-grade rocks: a case study on garnet– pyroxene granulites in southern Sri Lanka. Mineralogical Magazine, **55**, 17- 40.

Galli, A., Le Bayon, B., Schmidt, M.W., Burg, J.P., Caddick,M.J. & Reusser, E., 2010. Granulites and charnockites of the Gruf Complex: evidence for Permian ultra-high temperature metamorphism in the Central Alps. Lithos, **124**, 17-45.

Gallien, F., Mogessie, A., Bjerg, E., Delpino, S., Castro de Machuca, B., Thöni, M. & Klötzli, U., 2010. Timing and rate of granulite facies metamorphism and cooling from multi-mineralchronology on migmatitic gneisses, Sierras de La Huerta and Valle Fértil, NW Argentina. Lithos, 114, 229-252.

Geological Survey Department of Sri Lanka, 1996. Geological Map of Sri Lanka Colombo: Geological Survey Department of Sri Lanka. Scale 1:100000, sheets No16.

Hapuarachchi, D. J. A. C., 1968. Cordierite- and wollastonite-bearing rocks of south-western Ceylon. Geological Magazine, **105**: 317-324.

Harley, S. L., 1998. On the occurrence and characterization of ultrahightemperature crustal metamorphism. In: Treloar, P.J., O'Brien, P.J. (Eds.), What Drives Metamorphism and Metamorphic Relations?.Special Publications. Geological Society, London, 81-107.

Harley, S. L., 2004. Extending our understanding of Ultra high temperature crustal metamorphism. Journal of Mineralogical and Petrological Sciences, **99**, 140-158.

Harley, S. L., 2008. Refining the *P–T* records of UHT crustal metamorphism. Journal of Metamorphic Geology, **26**, 125-154.

Harley, S. L. & Hensen, B. J., 1990. Graphical analysis of *P–T–X* relations in granulite facies metapelites. In: Ashworth, J. R.,Brown, M. (Editors), Hightemperature metamorphism and crustal anatexis. The Mineralogical Society, Series 2. Mineralogical Society of Great Britain, Unwin Hyman, London, 19-56.

Harris, N., 1981. The application of spinel-bearing metapelitics to P/T determinations: an example from South India, Contributions to Mineralogy and Petrology, **6**, 229-233.

Henry, D. J., Guidotti, C. V. & Thomson, J. A., 2005. The Ti-saturation surface for low-to-medium pressure metapelitic biotites: Implications for geothermometry and Ti-substitution mechanism. American Mineralogist, **90**, 316-328.

Hensen, B. J., 1986. Theoretical phase relations involving cordierite and garnet revisited: the influence of oxygen fugacity on the stability of sapphirine and spinel in the system Mg–Fe–Al–Si–O. Contributions to Mineralogy and Petrology, **92**, 362-367.

Hensen, B. J., 1987. *P–T* grids for silica-undersaturated granulites in the systems MAS (n + 4) and FMAS (n +3): tools for the derivation of the *P–T* paths of metamorphism. Journal of Metamorphic Geology, **5**, 255-271.

Hiroi, Y., Yoshida, M.&Vitanage, P. W., 1987. Relict kyanite in the Highland and Southwest gneisses in Sri Lanka: evidence of prograde metamorphism and a characteristic in common with the Lützow-Holm Complex in East Antarctica. In: D. E. de S. Jayawardena, P. G. Cooray and K. Dahanayake (Editors), Precambrian Events in the Gondwana Fragments. Geological Society of Sri Lanka, Special.Publication, **3**. 28.

Hiroi, Y., Ogo, Y. & Namba, K., 1994.Evidence for prograde metamorphic evolution of Sri Lankan pelitic granulites, and implications for the development of continental crust. Precambrian Research, **66**, 245-263.

Holland, T. J. B. & Powell, R., 1996. Thermodynamics of order-disorder in minerals: II. Symmetric formalism applied to solid solutions. American Mineralogist, **81**, 1425-1437.

Holland, T. J. B. & Powell, R., 1998. An internally consistent thermodynamic dataset for phases of petrological interest. Journal of Metamorphic Geology**, 16**, 309-343.

Holdaway, M. J.&Lee, S. M., 1977.Fe-Mg cordierire stabiliry in high grade pelitic rocks based on experimental, theoretical and natural observations. Contributions to mineralogy and Petrology, **6**, 175-198

Kawakami, T. & Motoyoshi, Y., 2004.Timing of attainment of the spinel+quartz coexistence in garnet–sillimanite leucogneiss fromSkallevikshalsen, Lützow–Holm complex, East Antarctica. Journal of Mineralogical and Petrological Sciences, **99**, 311-319.

Kawasaki, T. & Motoyoshi, Y., 2007. Solubility of TiO_2 in garnet and orthopyroxene: Ti thermometer for ultrahigh-temperature granulites. In: Cooper, A.K., et al. (Ed.), Antarctica: A Keystone in a Changing World, USGS Open-File Report 2007-1047, Short Research Paper 038.

Kawasaki, T. Nakano, N. & Osanai, Y., 2011. Osumilite and a spinel+quartz association in garnet–sillimanite gneiss from Rundvågshetta, Lützow-Holm Complex, East Antarctica. Gondwana Research, **19**, 430-445.

Kelsey, D. E., 2008. On ultrahigh-temperature crustal metamorphism, Gondwana Research, **13**, 1-29.

Kehelpannala, K. V. W., 1997. Deformation of a high-grade gondwana fragment, Sri Lanka. Gondwana Research, **1**, 47-68.

Kehelpannala, K. V. W., 2003. Structural evolution of the middle to lower crust in Sri Lanka—a review. Journal of the Geological Society of Sri Lanka, **11**, 45-86.

Koziol, A. M. & Newton, R. C., 1988. Redetermination of the anorthite breakdown reaction and improvement of the plagioclase-garnet-Al_2SiO_5-quartz barometer. American Mineralogist, **73**, 216-223.

Kretz, R., 1983. Symbols for rock-forming minerals. American Mineralogists, **68**, 277-279.

Kriegsman, L. M.&Schumacher, J. C., 1999.Petrology of sapphirine-bearing and associated granulites from central Sri Lanka. Journal of Petrology, **40**, 1211–1239.

Kröner, A., Cooray, P. G. & Vitanage, P. W., 1991. Lithotectonic subdivision of the Precambrian basement in Sri Lanka. In: Körner,A. (Ed.), The Crystalline Crust of Sri

Lanka, Part-1. Summary of Research of the German-Sri Lankan Consortium. Geological Survey Department, Sri Lanka, Prof. Pap., **5**, 5-21.

Kröner, A., Kehelpannala, K. V. W. & Hegner, E., 2003. *ca*. 700–1000 Ma magmatic events and grenvillian-age deformation in Sri Lanka: relevance for rodinia supercontinent formation and dispersal, and Gondwana amalgamation. Journal of Asian Earth Sciences, **22**, 279-300.

Kröner, A., Rojas-Agramonte, Y., Kehelpannala, K. V. W., Zack, T., Hegner, E., Geng, H. Y., Wong, J. & Barth, M., 2012.Age, Nd–Hf isotopes, and geochemistry of the Vijayan Complex of eastern and southern Sri Lanka: A Grenville-age magmatic arc of unknown derivation, Precambrian Research, (Article in Press).

Loomis, T. P., 1972. Contact metamorphism of pelitic rocks by the Ronda ultramafic intrusion, southern Spain. Bull, Geological Society of America, **83**, 2449-2473.

Mathavan, V., Prame, W. K. B. N. & Cooray, P. G., 1999. Geology of the high grade Proterozoic terrains of Sri Lanka and the assembly of Gondwana: an update on recent developments. Gondwana Research, **2**, 237-250.

Mathavan, V. and Fernando & G. W. A. R., 2001.Reactions and textures in grossular–wollastonite–scapolite calc–silicate granulites from Maligawila, Sri Lanka: evidence for high-temperature isobaric cooling in the meta-sediments of the Highland Complex, Lithos, **59**, 217-232.

Milisenda, C. C., Leiw, T. C., Hofmann, A. W.& Kröner, A.,1988. Isotopic mapping of age provinces in Precambrian high grade terrains:Sri Lanka. Journal of Geology, **96**, 608-615.

Milisenda, C. C., Liew, T. C., Hofmann, A. W. &Kröner, H., 1994. Nd isotopic mapping of the Sri Lankan basement: update, and additional constraints from Sr isotopes. Precambrian Research, **66**, 95-110.

Morimoto, T., Santosh, M., Tsunogae, T. & Yoshimura, Y., 2004. Spinel+quartz association from the Kerala khondalites, southern India: evidence for ultrahigh-temperature metamorphism. Journal of Mineralogical and Petrological Sciences, **99**, 257-278.

Newton, R. C.& Haselton, H. T., 1981.Thermodynamics of the garnetplagioclase-Al_2SiO_5-quartz geobarometer. In R C Newton, A Navrotsky, and B.J Wood, Eds, Advances in physical geochemistry, **l**, 131-147.

Nichols, G. T., Berry, R. F. & Green, D. H., 1992. Internally consistent gahnitic spinel–cordierite–garnet equilibria in the FMASZn system: geothermobarometry and applications. Contributions to Mineralogy and Petrology, **111**, 362-377.

Ogo, Y., Hiroi, Y., Prame, K. B. N.&Motoyoshi, Y., 1992. A new insight of possible correlation between the Lutzow-Holm bay granulites (East Antarctica) and the Sri Lankan granulites. Resent progress in Antarctic Earth science, Ed: Yoshida et al., 75-86.

Osanai, Y., 1989. A preliminary report on saphirine / kornerupine granulite from Highland series, Sri Lanka.(Extended abstract), Seminar on recent advantages in Precambrian Geology of Sri Lanka, IFS Kandy, Sri Lanka.

Osanai, Y., Ando, K. T., Miyashita, Y., Kusachi, I., Yamasaki, T., Doyama, D., Prame, W.K.B.N., Jayatilake, S. & Mathavan, V., 2000. Geological field work in the southwestern and central parts of the Highland complex, Sri Lanka during 1998–1999, special reference to the highest grade metamorphic rocks. Journal of Geoscience, Osaka City University, **43**, 227-247.

Osanai, Y., Sajeev, K., Owada, M., Kehelpannala, K. V. W., Prame, W. K. B.&Nakano, N., 2003. Evolution of highest-grade metamorphic rocks from Central Highland Complex, Sri Lanka, Geological Survey and Mines Bureau, Sri Lanka, Centenary Publication, 25-31.

Osanai, Y., Sajeev, K., Owada, M., Kehelpannala, K. V. W., Prame, W. K. B. Nakano, N.&Jayatileke, S., 2006. Metamorphic evolution of ultrahigh-temperature and high-pressure granulites from Highland Complex, Sri Lanka. Journal of Asian Earth sciences, **28**, 20-37.

Powell, R. & Holland, T. J. B., 1999. Relating formulations of the thermodynamics of mineral solid solutions: activity modelling of pyroxenes, amphiboles and micas. American Mineralogist, **84**, 1-14.

Raase, P.&Schenk, V., 1994. Petrology of granulitefacies metapelites of the Highland Complex, Sri Lanka: implications for the metamorphic zonation and the PT path. In: M. Raith and S. Hoernes (Editors), Tectonic, Metamorphic and Isotopic Evolution of Deep Crustal Rocks, With Special Emphasis on Sri Lanka. Precambrian Research, **66**, 265-294.

Sandiford, N., Powell, R., Martin, S. F.&Perera, L. R. K., 1988.Thermal and baric evolution of garnet granulites from Sri Lanka. Journal of Metamorphic Geology, **6**, 351-364.

Santosh, M., Yokoyama, S., Biju-Sekhar, S. & Rogers, J.J.W., 2003. Multiple tectonothermal events in the granulite blocks of southern India revealed from EPMA dating: implications on the history of supercontinents. Gondwana Research **6**, 29–63.

Santosh, M. & Sajeev, K., Li, J. H., 2006. Extreme crustal metamorphism during Colombia supercontinent assembly: evidence from North China Craton. Gondwana Research, **10**, 256-266.

Sajeev, K. & Osanai, Y., 2004a.Ultrahigh-temperature metamorphism (1150 ^{0}C, 12 kbar) and multi-stage evolution of Mg, Al rich granulites from the central Highland Complex, Sri Lanka. Journal of Petrology, **45**, 1821-1844.

Sajeev, K. & Osanai, Y., 2004b. Osumilite and spinel+quartz from Sri Lanka: implications for UHT conditions and retrograde P–T path. Journal of Mineralogical and Petrological Sciences, **99**, 320-327.

Sajeev, K., Osanai, Y., Suzuki, S. & Kagami, H., 2003.Geochronological evidence for multistage-metamorphic events in ultrahigh-temperature granulites from central Highland Complex, Sri Lanka.Polar Geosciences, **16**,137-148.

Sajeev, K., Osanai, Y., Connolly, J. A. D., Suzuki, S., Ishioka, J., Kagami, H. & Rino, S., 2007. Extreme crustal metamorphism during a Neoproterozoic event in Sri Lanka, A study of dry mafi c granulites. Journal of Geology, **115**, 563-582.

Sajeev, K., Williams, I. S. & Osanai, Y., 2010. Sensitive high-resolution ion microprobe U-Pb dating of progradeand retrograde ultrahigh-temperature metamorphism as exemplified by Sri Lankan granulites. Geological Society of America, **38**, 971-974.

Schumacher, R & Faulhaber, S., 1994. Summary and discussion of P–T estimates from garnet–pyroxene–plagioclase–quartz-bearing granulite-facies rocks from Sri Lanka. Precambrian Research, **66**, 295-308.

Shabeer, K. P., Sajeev, K., Okudaira, T. & Santosh, M., 2002. Two-stage spinel growth in the high-grade metapelites of the Central Kerala Khondalite Belt:implication for prograde P-T path. Journel of Geosciences, Osaka City University, **45**, 29-43.

Shultere, J. & Bohlen, S., 1988. The stability of hercynite and hercynite-gahnite spinels in corundum- or quartz- bearing assemblage.Journal of Petrology, **30**, 1017-1031.

Stoddard, E. F., 1979. Zinc-rich hercynite in high-grade metamorphic rocks: a product of the dehydration of staurolite. American Mineralogist, **64**, 736-741.

Su, B. X., Zhang, H.F., Hu, Y., Santosh, M., Tang, Y. J. & Xiao, Y., 2012a.The genesis of mantle-derived sapphirine. American Mineralogist, 97, 856-863.

Su, B. X., Zhang, H. F., Deloule, E., Sakyi, P. A., Xiao, Y., Tang, Y. J., Hu, Y., Ying, J. F. & Liu, P. P., 2012b. Extremely high Li and low •^{7}Li signatures in the lithospheric mantle. Chemical Geology, **292-293**, 149-157.

Saxena, A., &Pandit, M. K., 2012.Geochemistry of Hindoli Group metasediments, SE Aravalli Craton, NW India: Implications for palaeoweathering and provenance, Journal of the Geological Society of India, **79,** 267-278.

Taj•manová, L., Connolly, J. A. D.& Cesare, B., 2009. A thermodynamic model for titanium and ferric iron solution in biotite. Journal of Metamorphic Geology, **27**, 153-165.

Taylor-jones, K. & Powel., R., 2010. The stability of saphirine + quatz: calculated phase equilibria in FEO-MgO-Al_2O_3-SiO_2-TiO_2-O. Journal of Metamorphic Geology, **28**, 615-633.

Tsunogae, T**.**, Santosh, M., Ohyama, H. & Sato, K., 2008.High-pressure and ultrahigh-temperature metamorphism at Komateri, northern Madurai Block, southern India. Journal of Asian Earth Sciences, **33**, 395-413.

Vielzeuf, D. & Holloway, J. R., 1988. Experimental determination of the fluid-absent melting relations in the pelitic system: consequences for crustal differentiation, Contributions to Mineralogy and Petrology. **98**, 257–276.

Vielzeuf, D. & Monte, J. M., 1994. Partial melting of metagreywackes; part 1, fluid -absent experiments and phase relationships, Contributions to Mineralogy and Petrology. **117**, 375–393.

Vitanage, P. W., 1972. Post-Precambrian uplifts and regional neotectonic movements in Ceylon (Sri Lanka). Proceedings of the 24th International Geolology Conference., Section 3: 642-654.

Voll, G.&Kleinschrodt, R., 1991. Sri Lanka: structural, magmatic and metamorphic development of a Gondwana fragment. In: A. Kröner (Editor), The Crystalline Crust of Sri Lanka, Part I. Summary of Research of the German-Sri Lankan Consortium, Geological Survey Department Sri Lanka, 22-51.

Waldbaum, D. R. & Thompson, J. B. J., 1969. Mixing properties of sanidine crystalline solutions: IV. Phase diagrams from equation of state. American Mineralogist, **54**, 1274-1298.

Waters, D., 1986. Metamorphic history of sapphirine-bearing and related magnesian gneisses from Namaqualand, South Africa. Journal of Petrology, **27**, 541-565.

Waters, D. J., 1991. Hercynite–quartz granulites: phase relations, and implications for crustal processes. European Journal of Mineralogy, **3**, 367-386.

Wells, P.D.A.&Richardson, S.W., 1980.In Caledonides of the British Isles--reviewed.(Eds. Harris, A. L., Holland, C. H. & Leake, B. E.)Geological Society of London.Special.Publication.**8**, 339-44.

White, R. W, Powell, R, Holland, T. J. B. & Worley, B. A., 2000. The effect of TiO_2 and Fe_2O_3 on metapelitic assemblages at greenschist and amphibolite facies conditions: mineral equilibria calculations in the system K2O-FeO-MgO-Al_2O_3-SiO_2-H_2O-TiO_2-Fe_2O_3. Journal of Metamorphic Geology, **18**, 497-511.

White, R. W., Powell, R. & Clarke, G. L., 2002. The interpretation of reaction textures in Fe-rich metapelitic granulites of the Musgrave Block, central Australia: constraints from mineral equilibria calculations in the system K_2O–FeO–MgO–Al_2O_3–SiO_2–H_2O–TiO_2–Fe_2O_3. Journal of Metamorphic Geology, **20**, 41-55.

White, R. W., Powell, R. & Holland, T. J. B., 2007.Progress relating to calculation of partial melting equilibria for metapelites. Journal of Metamorphic Geology, **25**, 511-527.

Zhang, H., Li, J., Liu, S., Li, W., Santosh, M. & Wang, H., 2012. Spinel+quartz-bearing ultrahigh-temperature granulites from Xumayao, Inner Mongolia Suture Zone, North China Craton: Petrology, phase equilibria and counterclockwise *P-T* path. Geosciences Frontiers, **3**, 603-611.

Figure captions

Fig. 1. Geological subdivisions of the Sri Lankan basement (after Cooray, 1994). Present sampling locality is shown by a star notation while reported UHT localities (**1**. Osanai, 1989 (>900 ^{0}C); **2**.Kriegsman and Schumacher, 1999 (830 ^{0}C); **3**.Sajeev and Osanai, 2004a (~950 ^{0}C) **4**.Sajeev and Osanai, 2004b, (1150 ^{0}C) **5**. Osanai et al, 2006 (>1000 ^{0}C); **6**. Sajeev et al, 2007 (~925 ^{0}C) by circles).

Fig. 2. Geological map of the area. The star corresponds to the sample locality. Modified from the published map of the Geological Survey Department of Sri Lanka (1996).

Fig. 3. (a) Porphyroblastic garnet in the cordierite-rich rock domain; (b) Hand specimen with porphyroblastic garnet surrounded by cordierite moat, compositional layering of the khondalite; (c) Alternance of khondalite and interbedded intermediate granulite layers; (d) Isoclinal folded khondalite together with intermediate granulites.

Fig. 4. (a) Spinel + quartz assemblage within garnet; (b) Back-scattered image of spinel + quartz assemblage; (c) Closer view of spinel + quartz assemblage; (d) Sillimanite corona around spinel; (e) Back-scattered image of sillimanite corona around spinel; (f) Skeletal sillimanite close to spinel within garnet; (g) Cluster of skeletal sillimanite around spinel in presence of quartz in garnet and large ilmenite grains; (h) Back-scattered image of tourmaline crystals within garnet; (i) Cordierite inclusions within rim and lower mantle of garnet; (j) Cordierite moat around porphyroblastic garnet; (k) Spinel + cordierire moat around garnet; (l) Back-scattered image of spinel + cordierite moat around garnet; (m) Spinel symplectite at the margin of sillimanite embedded in cordierite moats around garnet; (n) Back-scattered image of spinel symplectite at the margin of sillimanite; (o) Inclusion phases of medium grain

garnet; (p) Matrix minerals around coarse-grained garnet-bearing domains; (q) Matrix minerals of fine-grained garnet-bearing domains; (r) Matrix minerals of intermediate granulites interbedded with khondalites (Mineral abbreviations after Kretz, 1983).

Fig. 5. Chemical zoning pattern of spinel+quartz bearing garnet-porphyroblast, (a) Almandine component, (b) Grossular component, (c) Pyrope component, (d) Spessartite component.

Fig. 6. (a) Khondalite T-X(Fe_2O_3) pseudosection calculated in the NCKFMASHTMnO system at P = 8.0 kbar;(b) Khondalite P-T pseudosection calculated at X(Fe_2O_3) = 0.10; (c) Intermediate granulite T-X(Fe_2O_3) pseudosection calculated in the NCKFMASHTiMnO system at P = 8.0 kbar; (d) Intermediate granulite P-T pseudosection calculated at X(Fe_2O_3) = 0.01. Solution-phase models used in the calculations are: garnet – Gt(WPH): White et al. (2007); biotite – Bio(TCC): Tajcmanova *et al*. (2009); sapphirine – Sapp(Tp): Taylor-Jones and Powell (2010); ilmenite –Ilm(WHP); White et al. (2000); alkali-feldspar – San: Waldbaum and Thompson (1969); plagioclase – Pl(h): Newton *et al*. (1981); orthopyroxene – Opx(HP): Powell and Holland (1999); spinel – Sp(WPC): White et al. (2002); cordierite – hCrd: Holland and Powell (1998); clinopyroxene – Omph(HP): Holland and Powell (1996); amphibole – cAmph(DP): Diener *et al*. (2007); melt – melt (HP): White *et al*. (2007).

Fig. 7. P-T diagram showing the trajectory of the khondalite determined by conventional thermobarometric methods and pseudosections.

Fig. 8. Compositional diagram comparing spinel compositions of this study with other UHT terrains.1 - Kerala Khondalite belt, southern India, Morimoto et al. (2004; 8kbar, 950 ^{0}C), 2 - Skallevikshalsen, Lutzo-Holm Complex, East Antarctica, Kawakami and Motoyoshi (2004;

7.5 kbar, ~900 ^{0}C), 3 - Highland Complex, Sri Lanka, Sajeev and Osanai, (2004b; 7kbar, 850 ^{0}C), 4 - Jequie Block, Bahia, Brazil, Barbosa *et al*., (2006; ~8kbar, ~1000 ^{0}C), 5 - North China Craton, Santosh *et al*. (2006; 12 kbar, 900 ^{0}C), 6 - North China Craton, Santosh *et* al., (2006; 9kbar, 975 ^{0}C), 7 - Madurai Block, Southern India, Tsunogae *et a*l. (2008; ~9kbar, 1000 ^{0}C), 8 - Rundvagshetta, Lutzow-Holm Complex, East Antarctica, Kawasaki *et al*., (2011; 6.1 kbar, 830 ^{0}C), 9 - Mongolia Suture Zone (IMSZ) in the North China Craton (Zhang *et al*., 2012;>7.5 kbar, >975 ^{0}C), 10 - Mongolia Suture Zone (IMSZ) in the North China Craton (Zhang *et* al., 2012;>7.5 kbar, >975 ^{0}C), 11 - This study.

Table 1. Representative bulk chemical compositions of khondalite and Intermediate granulite

Sample	Khondalite	Intermediate granulite
(wt.%)		
SiO_2	57.27	56.82
TiO_2	0.68	0.63
Al_2O_3	20.24	14.82
FeO	10.03	11.45
MnO	0.18	0.21
MgO	3.70	7.96
CaO	2.44	5.08
Na_2O	2.67	1.33
K_2O	2.07	0.92
H_2O	0.25	0.43
Total	99.58	99.76
XMg	0.27	0.41
(ppm)		
Rb	175.80	74.40
Ba	205.00	143.80
Sr	105.90	120.50
Nb	6.30	5.30
Zr	207.60	126.10
Y	59.30	30.80
Zn	218.10	175.50
Cu	32.00	48.50
Ni	50.30	156.10
Cr	298.30	584.70
V	110.60	171.00
Sc	33.20	30.70
Th	44.00	15.00
U	4.30	1.30

Table 2. Representative electron microprobe analyses of spinel.

Textural Setting	Spl inclusions in Grt		Spl in the matrix	
Oxide wt%	Spl + Qtz	Corona-Sil	Symplectite-Sil	Isolated
SiO_2	0.09	0.07	0.20	0.09
TiO_2	0.08	0.00	0.02	0.08
Al2O_3	60.61	61.12	59.96	54.19
Cr_2O_3	0.80	0.20	0.71	6.27
FeO*	18.96	22.43	28.03	25.89
MnO	0.02	0.10	0.09	0.02
MgO	7.52	8.02	7.21	5.40
CaO	0.02	0.02	0.02	0.00
Na_2O	0.35	0.34	0.17	0.26
K_2O	0.03	0.01	0.00	0.00
ZnO	12.85	9.17	4.09	7.99
Total	101.31	101.46	100.49	100.19
Number of cations for 4 oxygens				
Si	0.002	0.002	0.005	0.003
Ti	0.002	0.000	0.000	0.002
Al	1.966	1.969	1.953	1.833
Cr	0.017	0.004	0.015	0.142
Fe	0.436	0.513	0.648	0.621
Mn	0.000	0.002	0.002	0.001
Mg	0.308	0.327	0.297	0.231
Ca	0.001	0.001	0.001	0.000
Na	0.019	0.018	0.009	0.014
K	0.001	0.000	0.000	0.000
Zn	0.261	0.185	0.083	0.169
Total cation	3.013	3.021	3.013	3.016
X_{Mg}	0.414	0.389	0.314	0.271
Cr#	0.009	0.002	0.008	0.072

FeO*: total Fe as FeO Corona-Sil: spinel surrounded by sillimanite
Symplectite-Sil: symplectitic spinel at the margins of sillimanite
Spl + Qtz: Spinel in contact with Qtz isolated: Isolated spinel in the matrix

Table 3

Table. 3 Representative electron microprobe analyses of garnet, cordierite, biotite, sillimanite, feldspar, ilmenite and tourmaline.

Mineral	Garnet			Cordierite		Biotite			Sillimanite			Orthoclase		Plaioclase	Ilmenite		Tourmaline
Textural setting	core	mantle	rim	in moat around Grt	inclusions in Grt rim	inclusions in Grt	contact with Spl+Qtz in Grt	contact with Grt rim	corona around Spl	inclusions in Grt	matrix	contact with Spl+Qtz in Grt	contact with Sil		contact with Grt rim	inclusions in Grt	inclusions in Grt
SiO_2	38.47	38.45	38.69	48.97	49.21	37.38	37.43	38.95	37.09	37.09	37.14	64.04	63.78	60.36	0.08	0.06	43.21
TiO_2	0.03	0.05	0.02	0.03	0.02	3.54	5.92	3.02	0.03	0.03	0.07	0.04	0.05	0.04	51.69	51.01	0.02
Al_2O_3	22.27	22.36	21.73	33.00	32.97	15.60	16.25	16.31	62.19	62.32	61.52	18.48	18.68	24.07	0.06	0.06	33.13
Cr_2O_3	0.08	0.07	0.03	0.05	0.04	0.40	0.05	0.00	0.18	0.17	0.35	0.04	-	-	0.15	0.11	0.32
FeO*	30.10	29.15	29.41	5.84	5.56	13.58	9.67	8.49	0.64	0.31	0.30	0.13	0.11	0.05	45.93	46.37	5.77
MnO	1.28	0.69	0.57	0.01	0.06	0.02	0.00	0.02	0.00	-	-	-	0.01	-	0.25	0.31	0.07
MgO	8.34	9.13	9.10	10.26	10.00	15.25	15.75	19.02	0.05	0.02	0.03	0.02	0.00	0.03	1.29	1.31	4.09
CaO	0.95	1.12	0.91	0.01	0.02	0.06	0.02	0.01	0.00	0.01	0.02	0.09	0.12	6.01	-	-	0.51
Na_2O	0.00	0.00	0.03	0.06	0.05	0.08	0.45	0.04	-	0.01	0.02	1.17	1.45	7.78	-	-	0.13
K_2O	0.02	0.01	0.00	0.02	0.01	9.74	9.44	9.76	-	-	0.01	14.75	14.31	0.76	-	-	0.61
ZnO	0.05	0.08	0.12	-	0.00	0.12	0.18	0.12	0.14	-	-	0.09	-	-	-	0.01	0.02
Total	101.6	101.1	100.6	98.3	97.9	95.8	95.2	95.8	100.3	100.0	99.5	98.8	98.5	99.1	99.5	99.2	87.9
Oxygen Number		12		18			22			5		8		8	3		30
Si	2.955	2.949	2.984	5.018	4.990	5.532	5.464	5.596	1.002	1.003	1.010	2.984	2.976	2.715	0.002	0.002	8.233
Ti	0.002	0.003	0.001	0.001	0.003	0.394	0.650	0.327	0.001	0.001	0.001	0.001	0.002	0.001	0.982	0.975	0.003
Al	2.016	2.021	1.975	3.938	3.964	2.720	2.796	2.762	1.980	1.986	1.972	1.015	1.027	1.276	0.002	0.002	7.440
Cr	0.005	0.004	0.002	0.003	0.004	0.047	0.005	-	0.004	0.004	0.007	0.001	-	0.000	0.003	0.002	0.047
Fe	1.934	1.870	1.897	0.477	0.497	1.681	1.180	1.020	0.015	0.007	0.007	0.005	0.004	0.002	0.970	0.985	0.919
Mn	0.084	0.045	0.037	0.001	0.001	0.003	-	0.003	-	-	-	-	-	-	0.006	0.007	0.012
Mg	0.955	1.044	1.045	1.569	1.557	3.363	3.426	4.073	0.002	0.001	0.001	0.001	-	0.002	0.049	0.050	1.160
Ca	0.078	0.092	0.075	0.002	0.001	0.009	0.003	0.002	-	-	0.001	0.005	0.006	0.289	-	-	0.103
Na	0.001	0.001	0.005	0.001	0.012	0.022	0.128	0.012	-	-	0.001	0.106	0.131	0.678	-	-	0.048
K	0.002	0.001	-	-	0.003	1.840	1.758	1.788	-	-	-	0.877	0.852	0.044	-	-	0.149
Zn	0.003	0.004	0.007	0.001	-	0.013	0.019	0.013	0.003	-	-	0.003	-	-	-	-	0.003
Total cation	8.034	8.036	8.029	11.011	11.031	15.622	15.429	15.596	3.006	3.002	3.000	4.998	4.999	5.007	2.014	2.022	18.118
Alm	0.621	0.598	0.609	-	-	-	-	-	-	-	-				-	-	-
Spe	0.028	0.015	0.013	-	-	-	-	-	-	-	-				-	-	-
Pyr	0.324	0.355	0.353	-	-	-	-	-	-	-	-				-	-	-
Grs	0.010	0.012	0.009	-	-	-	-	-	-	-	-				-	-	-
An														0.286			
Or												0.888	0.861				
X_{Mg}	0.331	0.358	0.355	0.767	0.758	0.667	0.744	0.800							0.048	0.048	0.558
Fe^{+2}*	0.105	0.111	0.092	-	-	-	-	-	-	-	-				0.920	0.914	-
Fe^{+3}*	1.830	1.760	1.805	-	-	-	-	-	-	-	-				0.039	0.062	-

*: based on stoichiometry; Alm: Almandine content; Spe: Spassartine content; Pyr: Pyrope content; Grs: Grossular content; An: Anorthite content

Table 4

Table 4. Conventional thermobarometric data calculated for the khondalite

Mineral Compositions	Si	Ti	Mg	Fe^{2+}	Mn	Ca	Na	K	Zn	Nominal T	Nominal P	Calculated P (kbar)	Calculated T (°C)	Reference*
Peak conditions										800		7.3	860	{1}, {2}
Garnet	2.995	0.0015	1.003	1.850	0.400	0.780				825		7.7		{1}
Plagioclase						0.289	0.678	0.044		850		8.0		{1}
										875		8.4		{1}
Biotite		0.650	3.426	1.180									828	{3}
		0.650	3.426	1.062									834	{3}
		0.650	3.426	0.944									841	{3}
Isobaric cooling														
Garnet			1.040	1.870	0.330									
Spinel			0.330	0.520					0.180	810		7.7		{4}
										830		8.2		{4}
Isothermal decompression														
Garnet			1.040	1.900	0.040	0.070								
Cordierite			1.570	0.480						750		7.2		{5}
Spinel			0.297	0.628						780		7.2		{5}
												6.6		{6}
												6.6		{6}
											6		761	{7}
											7		766	{7}
											8		772	{7}
													768	{8}
Biotite		0.327	4.073	1.020									770	{3}
		0.327	4.073	1.020									777	{3}

*{1} Grt-Sil-Plag-Qtz geobarometer, (Koziol and Newton, 1988); {2} Ti in Grt geothermometer (Kawasaki and Motoyoshi, 2007); {3} Ti in Biotite geothrmometer (Henry et al., 2005); {4} Grt-Sil-Spl-Qtz geobarometer, (Nicholson et al., 1992); {5} Grt-Cor-Sil geobarometer (Holdway and Lee (1997); {6} Grt-Cor-Sil geobarometer (Wells and Richardson, 1980); {7} Grt-Crd geothermometer (Bhattacharya et al., 1988); {8} Spl-Crd geothermometer (Das et al, 2003)

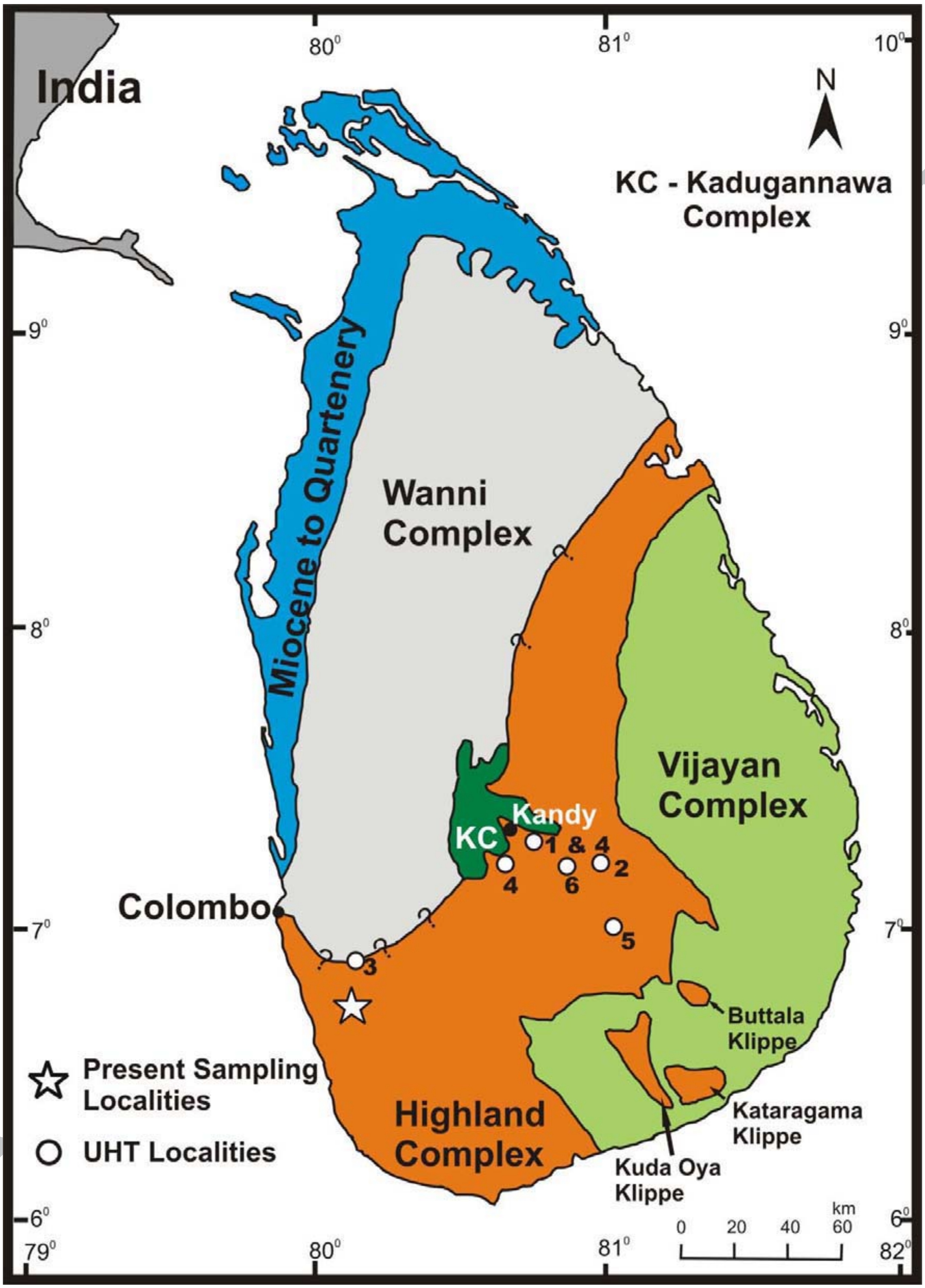
India
N
KC - Kadugannawa Complex
Miocene to Quartenery
Wanni Complex
Vijayan Complex
KC
Kandy
1 & 4
4
6
2
5
3
Colombo
Buttala Klippe
Kataragama Klippe
Kuda Oya Klippe
Highland Complex
Present Sampling Localities
UHT Localities
80°
81°
10°
9°
8°
7°
6°
79°
82°
km
0
20
40
60

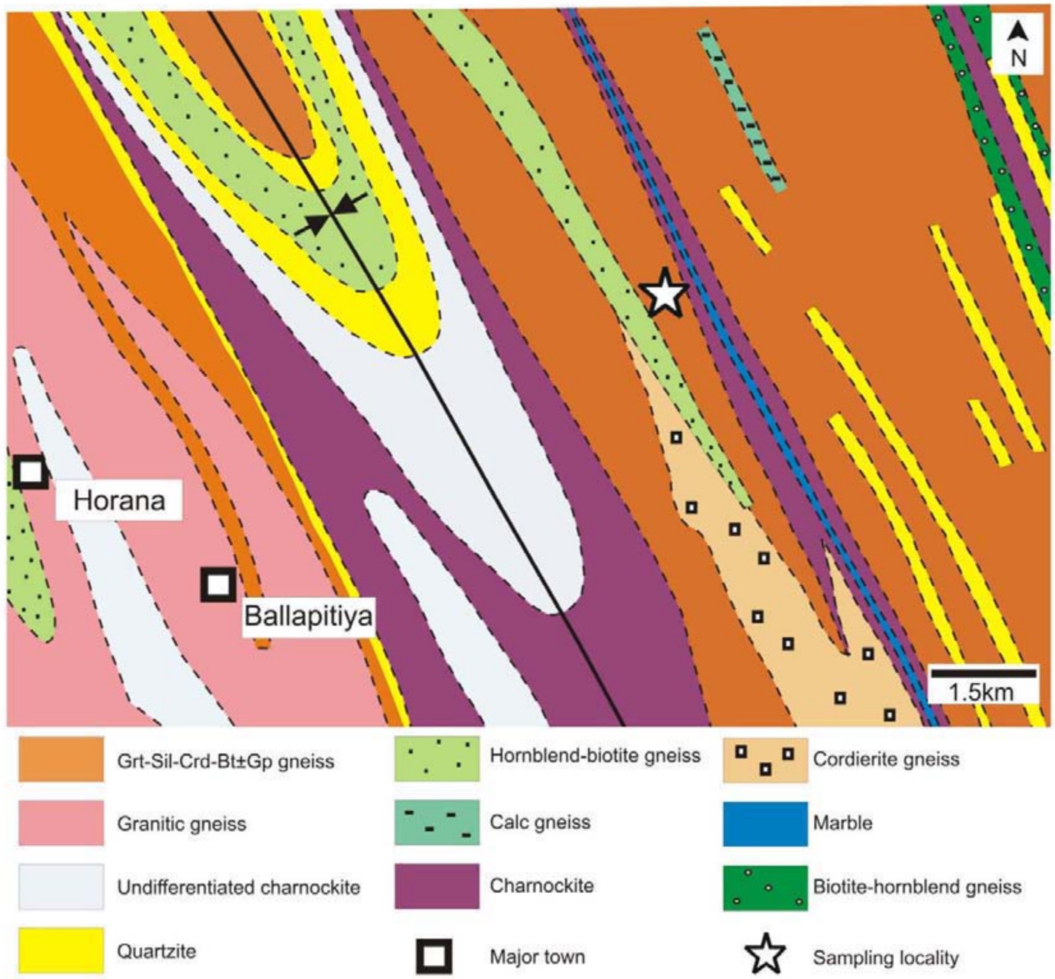
N
Horana
Ballapitiya
1.5km
Grt-Sil-Crd-Bt±Gp gneiss
Granitic gneiss
Undifferentiated charnockite
Quartzite
Hornblend-biotite gneiss
Calc gneiss
Charnockite
Major town
Cordierite gneiss
Marble
Biotite-hornblend gneiss
Sampling locality

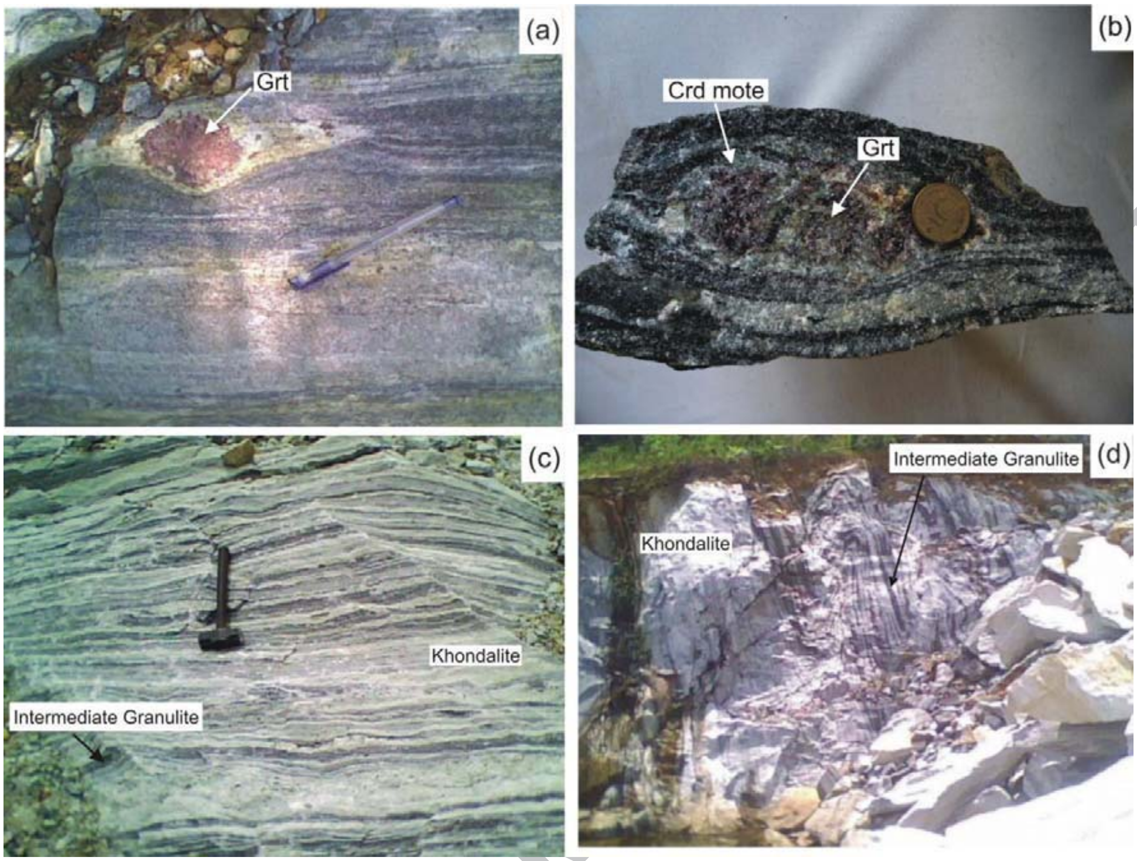
(a)
Grt
(b)
Crd mote
Grt
(c)
Khondalite
Intermediate Granulite
(d)
Intermediate Granulite
Khondalite

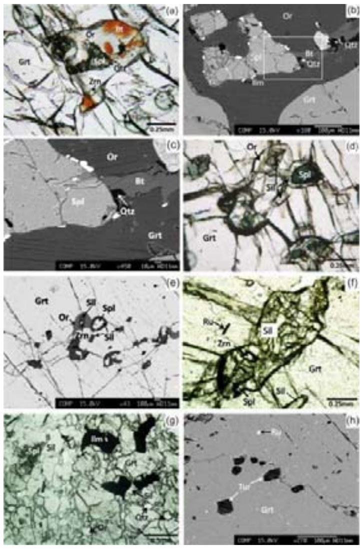

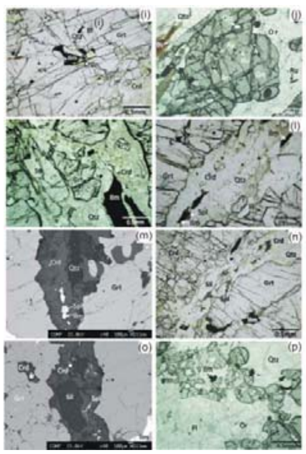

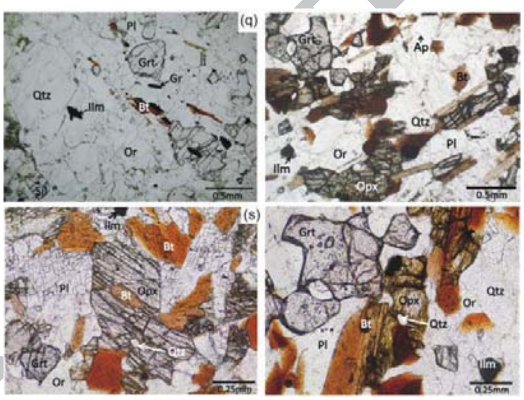
(q)
Pl
Grt
Qtz
Ilm
Bt
Or
0.5mm
Ap
Opx
(s)
0.25mm

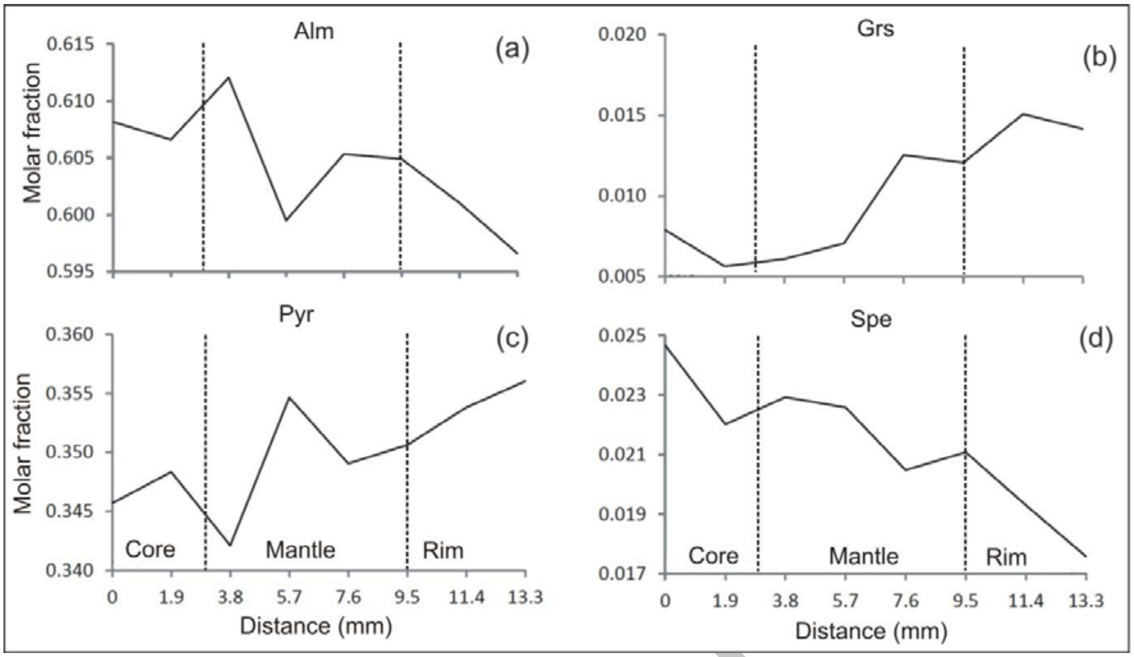
Alm
(a)
Molar fraction
0.615
0.610
0.605
0.600
0.595
Grs
(b)
0.020
0.015
0.010
0.005
Pyr
(c)
Molar fraction
0.360
0.355
0.350
0.345
0.340
Core
Mantle
Rim
0
1.9
3.8
5.7
7.6
9.5
11.4
13.3
Distance (mm)
Spe
(d)
0.025
0.023
0.021
0.019
0.017
Core
Mantle
Rim
0
1.9
3.8
5.7
7.6
9.5
11.4
13.3
Distance (mm)

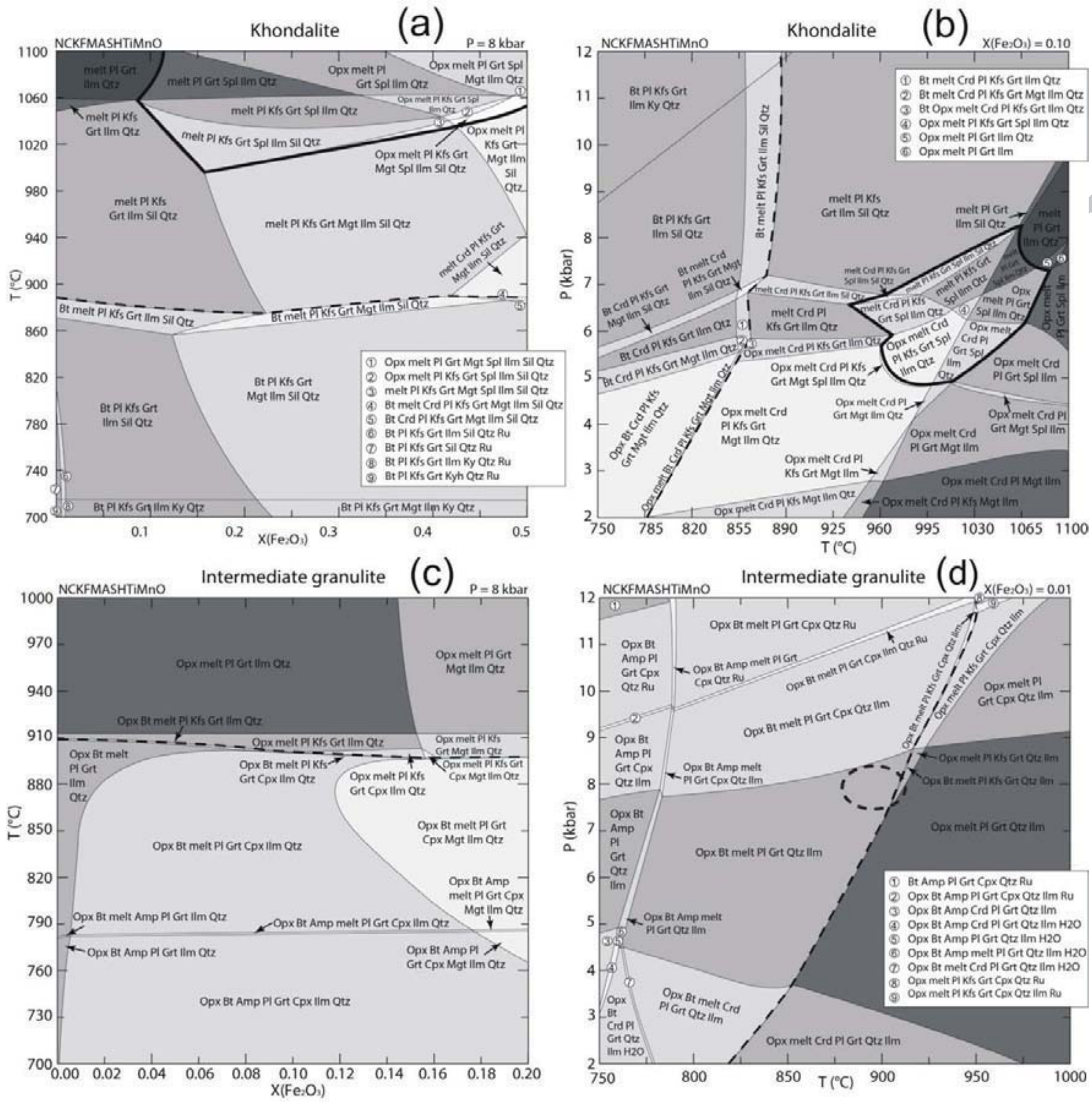

	mol %										
	SiO2	TiO2	Al2O3	Fe2O3	FeO	MnO	MgO	CaO	Na2O	K2O	H2O
Khondalite	62.83	0.56	13.09	0.92	8.28	0.17	6.06	2.87	2.84	1.45	0.92
Intermediate granulite	58.91	0.49	9.05	0.00	9.93	0.19	12.30	5.64	1.34	0.61	1.49

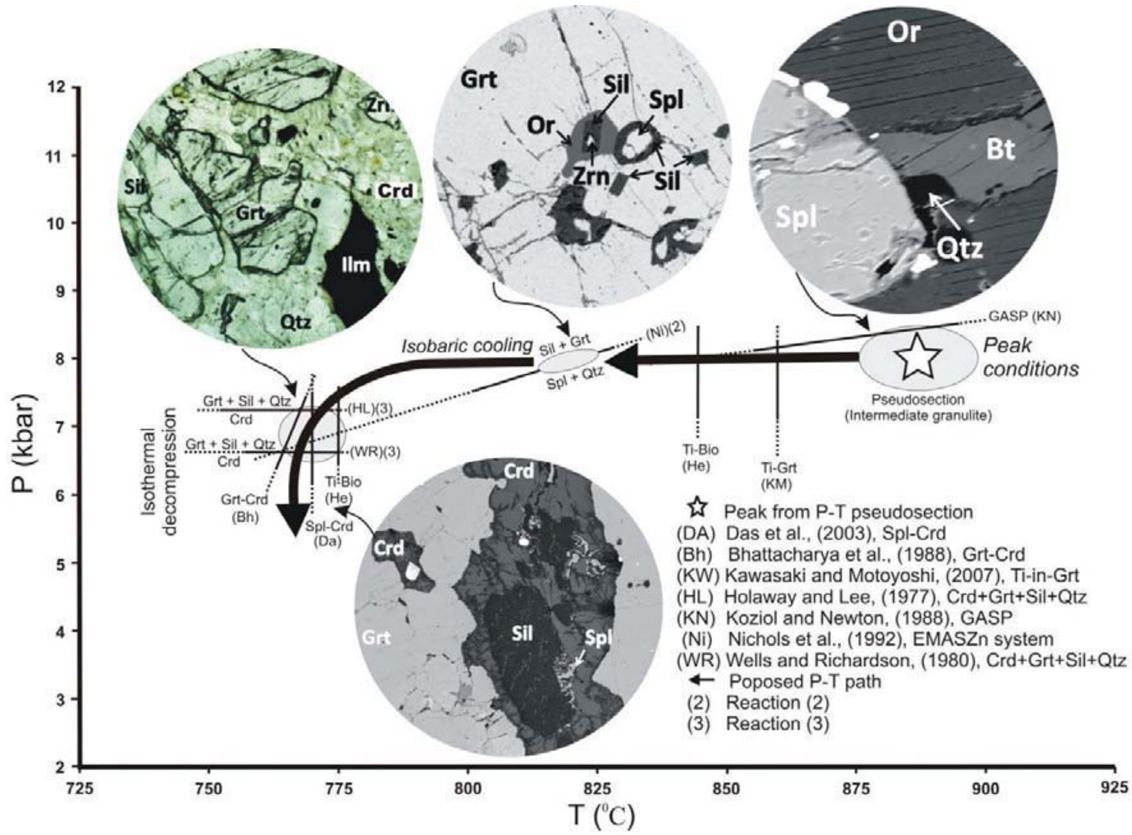

P (kbar)
T (°C)
Isobaric cooling
Isothermal decompression
Peak conditions
Pseudosection (Intermediate granulite)
GASP (KN)
Sil + Grt
Spl + Qtz
(Ni)(2)
Grt + Sil + Qtz
Crd
(HL)(3)
(WR)(3)
Grt-Crd (Bh)
Spl-Crd (Da)
Ti-Bio (He)
Ti-Grt (KM)
Peak from P-T pseudosection
(DA) Das et al., (2003), Spl-Crd
(Bh) Bhattacharya et al., (1988), Grt-Crd
(KW) Kawasaki and Motoyoshi, (2007), Ti-in-Grt
(HL) Holaway and Lee, (1977), Crd+Grt+Sil+Qtz
(KN) Koziol and Newton, (1988), GASP
(Ni) Nichols et al., (1992), EMASZn system
(WR) Wells and Richardson, (1980), Crd+Grt+Sil+Qtz
Poposed P-T path
(2) Reaction (2)
(3) Reaction (3)

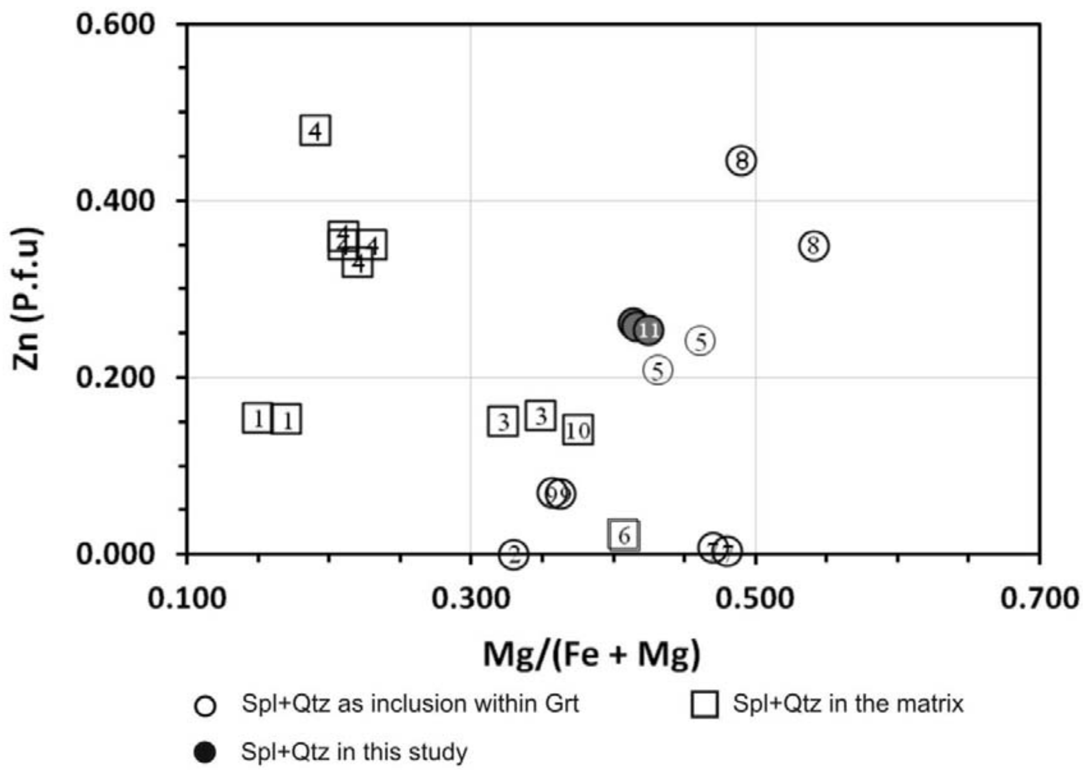

0.600
0.400
0.200
0.000
0.100
0.300
0.500
0.700
Zn (P.f.u)
Mg/(Fe + Mg)
Spl+Qtz as inclusion within Grt
Spl+Qtz in the matrix
Spl+Qtz in this study

Highlights

- We show a natural field example for difficulty of using Spl+Qtz as typical UHT assemblage Spl+Qtz
- We have model the Spl+Qtz bearing pelitic granulite and associated intermediate granulite using pseudosections
- We have correlated the stability of Spl+Qtz assemblage this study and previous studies
- We have obtained a retrograde P-T trajectory followed by the rock using pseudosections and conventional thermobarometry.